Properties of an Inwardly Rectifying ATP-sensitive K^+ Channel in the Basolateral Membrane of Renal Proximal Tubule

Ulrich R. Mauerer,* Emile L. Boulpaep,* and Alan S. Segal*‡

From the *Department of Cellular and Molecular Physiology, Yale University School of Medicine, New Haven, Connecticut 06520; and ‡Department of Medicine, University of Vermont, Burlington, Vermont 05401

ABSTRACT The potassium conductance of the basolateral membrane (BLM) of proximal tubule cells is a critical regulator of transport since it is the major determinant of the negative cell membrane potential and is necessary for pump-leak coupling to the Na^+,K^+-ATPase pump. Despite this pivotal physiological role, the properties of this conductance have been incompletely characterized, in part due to difficulty gaining access to the BLM. We have investigated the properties of this BLM K^+ conductance in dissociated, polarized *Ambystoma* proximal tubule cells. Nearly all seals made on *Ambystoma* cells contained inward rectifier K^+ channels ($\gamma_{slope,\,in}$ = 24.5 ± 0.6 pS, $\gamma_{chord,\,out}$ = 3.7 ± 0.4 pS). The rectification is mediated in part by internal Mg^{2+}. The open probability of the channel increases modestly with hyperpolarization. The inward conducting properties are described by a saturating binding–unbinding model. The channel conducts Tl^+ and K^+, but there is no significant conductance for Na^+, Rb^+, Cs^+, Li^+, NH_4^+, or Cl^-. The channel is inhibited by barium and the sulfonylurea agent glibenclamide, but not by tetraethylammonium. Channel rundown typically occurs in the absence of ATP, but cytosolic addition of 0.2 mM ATP (or any hydrolyzable nucleoside triphosphate) sustains channel activity indefinitely. Phosphorylation processes alone fail to sustain channel activity. Higher doses of ATP (or other nucleoside triphosphates) reversibly inhibit the channel. The K^+ channel opener diazoxide opens the channel in the presence of 0.2 mM ATP, but does not alleviate the inhibition of millimolar doses of ATP. We conclude that this K^+ channel is the major ATP-sensitive basolateral K^+ conductance in the proximal tubule.

KEY WORDS: ion channel • kidney • patch-clamp • sulfonylurea • epithelia

INTRODUCTION

The ability of the renal proximal tubule to maintain homeostatic electrolyte and water reabsorption in the face of drastic changes in dietary solute and water intake and renal hemodynamics implies that transtubular ion transport is tightly regulated. Proximal tubule potassium channels, particularly in the basolateral membrane (BLM),[1] play pivotal physiologic roles in the regulation of membrane voltage, potassium recycling, and ultimately in transepithelial solute and water reabsorption. That the basolateral membrane potential of a proximal tubule cell is dominated by the BLM K conductance is well established (Sackin and Boulpaep, 1983). The Na^+,K^+-ATPase pump in the BLM provides the energy that makes ion transport thermodynamically favorable, but continuous operation of the pump requires there be a K^+ exit pathway. The BLM K conductance provides such a pathway and thus steady state intracellular K activity can be maintained in the face of large transcellular fluxes of salt and water (Sackin and Boulpaep, 1983). Since a major portion of the transcellular Na^+ flux is reabsorbed across the BLM by the action of the Na^+,K^+-ATPase, a population of BLM K^+ channels working in concert with the pump would allow K^+ to recycle in a regulated fashion. Moreover, hyperpolarization secondary to the opening of BLM K^+ channels enhances the driving force for electrogenic apical Na^+ entry and basolateral Cl^- efflux, resulting in net NaCl reabsorption.

The *Ambystoma* proximal tubule exhibits a large K^+ conductance in the basolateral membrane (Siebens and Boron, 1987; Sackin and Boulpaep, 1981) that has been shown macroscopically to be sensitive to barium and pH. However, previous studies of the "macroscopic" BLM K^+ conductance (Boulpaep, 1976) lack the resolution to distinguish whether there is one population of imperfectly selective K^+ channels or a set of highly selective K^+ channels coexisting with a population of nonselective cation channels. More recent "microscopic" single-channel patch-clamp studies of BLM K^+ channels have shown diversity in both experimental design and findings (Tsuchiya et al., 1992; Hunter, 1991; Parent et al., 1988; Kawahara et al., 1987; Sackin and Palmer, 1987; Gögelein and Greger, 1987*a*, 1987*b*),

Address correspondence to Alan S. Segal, Department of Medicine, University of Vermont, 55A South Park Drive, Colchester, VT 05446. Fax: 802-656-8915; E-mail: asegal@zoo.uvm.edu

[1]*Abbreviations used in this paper:* BLM, basolateral membrane; c/a, cell-attached (patch); I-V, current–voltage; i/o, inside-out (patch); KCO, K channel opener; nP_o, channel activity represented as the product of the minimum number of channels (n) times the open probability (P_o) of the channel; SUR, sulfonylurea receptor.

so a clear consensus has been elusive and details of the properties and regulation are lacking.

We have now characterized the properties and regulation (see Mauerer et al., 1998) of the principal K^+ channel in the BLM in a preparation of dissociated yet polarized *Ambystoma* proximal tubule cells (Segal et al., 1996). Inwardly rectifying, ATP-sensitive K^+ channels were present in >95% of recordings from the BLM, each containing from 2 to >25 K_{ATP} channels/patch. Although the regulation of this proximal tubule BLM K^+ channel is similar to that of recently cloned K_{ATP} channels in the apical membrane of the distal nephron (ROMK1 and ROMK2), there are important differences, and ROMK has not been found in the proximal tubule (Chepilko et al., 1995; Zhou et al., 1994; Lee and Hebert, 1995; Boim et al., 1995; Ho et al., 1993). The studies reported in this paper and the companion paper elucidate the properties and the regulation, respectively, of the major K^+ channel underlying the BLM K conductance that is coupled to transport in the proximal tubule.

MATERIALS AND METHODS

Solutions and Drugs

The compositions of the solutions used are summarized in Table I. After titration to pH 7.5 (710A; Orion Research, Boston, MA), sucrose was added to adjust the osmolality of the solutions (3MO; Advanced Instruments Inc., Needham Heights, MA). To determine channel conductance as a function of $[K^+]$, sucrose was added to the standard pipette KCl to maintain osmolality. Chemicals used were of the highest quality and obtained from Sigma Chemical Co. (St. Louis, MO), except thallium acetate (Aldrich Chemical Co., Milwaukee, WI), diazoxide (Calbiochem Corp., La Jolla, CA), ATPγS, and ADP (Boehringer-Mannheim Biochemicals, Indianapolis, IN). Nucleotides were prepared fresh daily as 20–50-mM stocks in bath solution. Glibenclamide was dissolved in DMSO (100 mM stock).

Cell Preparation

Dissociated proximal tubule cells were isolated from amphibian kidneys as previously described (Segal et al., 1996). Briefly, aquatic phase *Ambystoma tigrinum* kept at 4°C were killed by submersion in 0.2% tricaine methanesulfonate. The kidneys were rapidly removed and placed in iced HEPES-buffered NaCl at pH 7.5 (solution *a*). The adventitial tissue was removed by hand dissection, and the renal tissue was cut into 1–2 mm^3 pieces and incubated in collagenase-dispase (0.2 U/ml of collagenase; Boehringer-Mannheim Biochemicals) on a gyratory shaker for 60 min at 22°C. The enzyme reaction was stopped by washing with Ca^{2+}- and Mg^{2+}-free NaCl (solution *b*). The cells were then mechanically dispersed into suspension by repeated trituration, and a pellet was obtained by centrifugation at ~1,600 rpm for 3 min. Finally, the cells were resuspended in 2.5 ml NaCl (solution *a*) in a 35-mm culture dish, and stored at 4°C until use. The dissociated proximal tubule cells can retain their epithelial polarity for up to 14 d (Segal et al., 1996). Cells were used for experiments from 2 to 12 d after dissociation. Representative cells as seen under light microscopy (Fig. 1 *A*) and scanning electron microscopy (Fig. 1 *B*) are shown (for details of methods see Segal et al., 1996).

Electrophysiology

A 5-μl aliquot of cell suspension in NaCl storage solution (solution *a*) was placed on a Cell-Tak™-coated glass coverslip in a re-

TABLE I

Solutions

	a NaCl Ringer	*b* Ca^{2+}/Mg^{2+}-free Ringer	*c* NaCl recording solution	*d* KCl recording solution	*e* Mg-free KCl	*f* KCl 200 nM Mg^{2+}	*g* Tl^+ pipette solution	*h* 2 mM Cl^- K solution	*i* KCl salt dilution
Na^+	95.9	98.5	95	2.5	2.5	2.5	5		2.5
K^+	2.5	2.5	2.5	95	95	95		95	14
Cl^-	98.1	92.5	94.5	94.5	92.5	96.1	2	2	13.5
Ca^{2+}	1.8								
Mg^{2+} (added, mM)	1		1	1		0.81	1	1	1
Mg^{2+} (free, nM)						200			
Tl^+							90		
$Acetate^-$							90	90	
HEPES	5	5	5	5	5	5	5	5	5
$HEPES^-$	5	5	5	5	5	5	5	5	5
EGTA			1	1			1	1	1
EDTA		1			8	8			
$H_2PO_4^-$	0.1	0.1							
HPO_4^{2-}	0.4	0.4							
Dextrose	2	2							
pH (titrand)	7.5 (NaOH)	7.5 (NaOH)	7.5 (NaOH)	7.5 (KOH)	7.5 (KOH)	7.5 (KOH)	7.5 (NaOH)	7.5 (KOH)	7.5 (KOH)
Osmolality	200	200	200	200	200	200	200	200	200

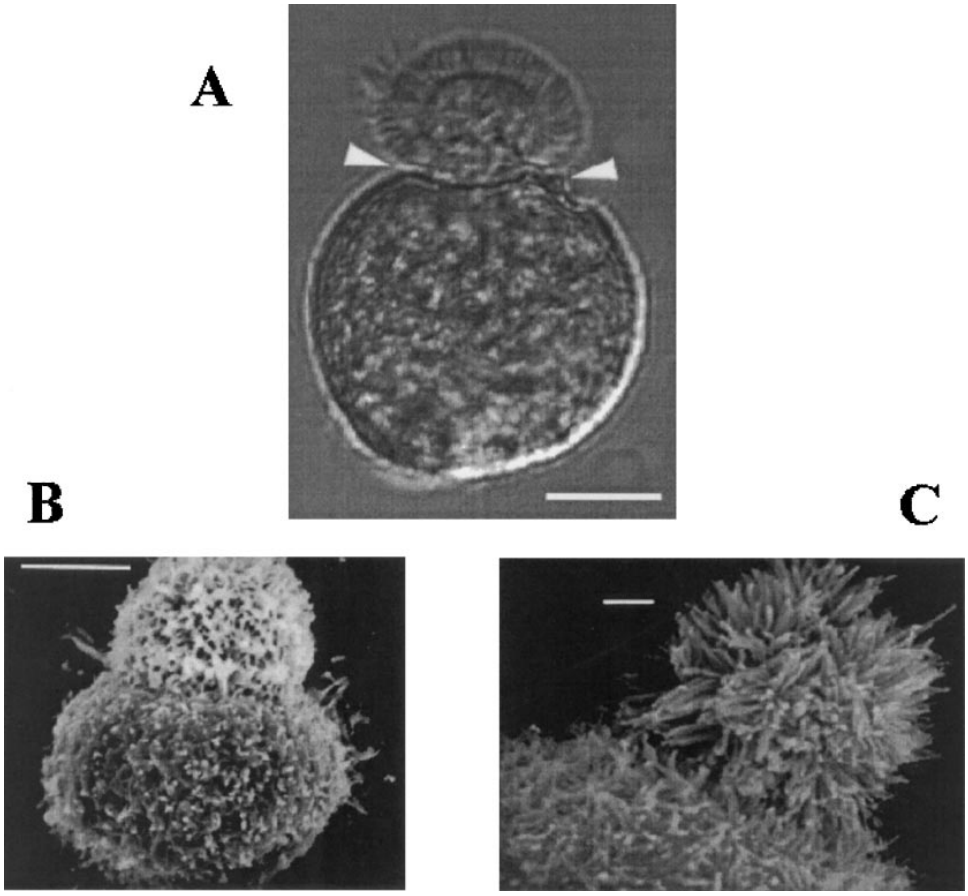

FIGURE 1. Dissociated *Ambystoma* proximal tubule cells retain epithelial cell polarity. (*A*) Light photomicrograph of a single dissociated *Ambystoma* proximal tubule cell shows distinct apical and basolateral membrane surfaces. The apical surface of these bilobated cells is the smaller lobe with a microvillar brush border. The robust cytoskeleton of these cells includes an actin-rich "waist-band" (*arrowheads*) between the two membrane domains that is important in retention of epithelial polarity. Giga-ohm seals can be made on both surfaces. Scale bar, 10 μm. (*B* and *C*) Scanning electron micrographs showing the sharp transition between the membrane domains and the detailed topology of the apical surface invested with its microvillar brush border, and the basolateral surface with its folds and projections. Scale bars: 10 μm in *B*, 1 μm in *C*.

cording chamber of our design (RC-5/25; Warner Instruments, Hamden, CT) mounted on an inverted microscope (Olympus IM; Olympus America, Inc., Melville, NY). The chamber has a bath volume of 500 μl, and solutions are perfused directly into an input multiplexer on the chamber at a gravity-driven flow rate of ~10 ml/min.

Nonadherent cells were washed off the coverslip with the recording solution (either Ca^{2+}-free NaCl, solution *c*, or KCl, solution *d*, unless otherwise noted) and the cells were visualized under Hoffman modulation optics (Modulation Optics, Greenvale, NY). Proximal tubule cells were readily recognized by their characteristic morphology (see Fig. 1; Segal et al., 1996). An individual proximal tubule cell was selected for an experiment only if it fulfilled the following criteria (Segal et al., 1996): (*a*) distinctly bilobated structure, (*b*) clearly defined brush border sharply delimited on the apical surface, (*c*) relatively smooth appearing basolateral membrane, and (*d*) absence of large vacuoles.

Patch clamp. The standard configurations for single-channel and whole-cell tight seal patch-clamp technique (Hamill et al., 1981) were used to record channel currents from the BLM. Patch pipettes were fabricated from borosilicate glass capillaries (Warner Instruments, Hamden, CT) on a two-step puller (PP-83; Narishige Co., Ltd, Tokyo, Japan), coated with Sylgard 184™ (Dow-Corning Corp., Midland, MI) to within 200 μm of the tip, and fire-polished just before use. When filled with KCl, the open tip pipette resistance was 3–8 MΩ when placed in the initial bath solution. A hydraulic micromanipulator (Narishige) was used to guide the patch microelectrode to the BLM of the cell. High resistance giga-ohm seals (up to 50 GΩ) were obtained on the BLM in ~75% of attempts by applying gentle suction to the pipette just after it touched the cell membrane. To achieve the whole-cell configuration, further suction was applied to rupture the cell-attached patch. Data have not been corrected for liquid-junction potentials since for most solutions they were <4 mV when measured as follows: the bath Ag-AgCl ground electrode was connected to the control KCl bath through a 3% agar bridge made of KCl pipette solution. A low resistance (<1 MΩ) pipette filled with 3 M KCl was placed in a KCl bath and the DC offset was adjusted to 0 mV in zero current clamp. The liquid-junction potentials were measured as the voltage offset resulting when the control KCl bath was replaced by the test solution. Low [Cl] solutions in which 90% of Cl^- was replaced by $aspartate^-$ had a liquid-junction potential of 13.3 mV.

Voltage-clamped membrane currents were amplified (and zero current-clamp membrane potentials were measured) with an EPC-7 patch-clamp amplifier (Medical Systems, Greenvale, NY) controlled by a PDP 11/23 computer (Digital Equipment Corp., Maynard, MA). The current (filtered at 10 kHz) and voltage outputs of the EPC-7 were digitized at 44.1 kHz using a modified pulse code modulator (501ES; Sony Corp., Tokyo, Japan), and stored on videotape (SL-HF300; Sony Corp.). Whole-cell membrane currents were also digitized at 250 samples/s (Cheshire A/D; Indec, Sunnyvale, CA) and stored directly on computer disk. Signals were monitored on an oscilloscope (205; Hameg Instruments, Inc., Frankfurt, Germany) and strip-chart recorder (220; Brush, Cleveland, OH). All experiments were carried out at room temperature (20–22°C).

Data Analysis

Current data were played back and low pass filtered at 400 Hz (902LPF eight-pole Bessel filter; Frequency Devices Inc., Haver-

hill, MA), digitized at 1,000 samples/s, and stored on the PDP-11/23. In some cases, currents were filtered at 40 Hz and digitized at 100 samples/s for current binning and averaging analysis. Datafiles were transferred to a Pentium computer (Gateway 2000, North Sioux City, SD) via Kermit (Columbia University, NY) for analysis. Custom software for data acquisition and analysis was written in our laboratory using BASIC-23, AxoBASIC 1.0 (Axon Instruments, Foster City, CA), and Matlab 4.0 (The Mathworks, Natick, MA).

Channel activity (nP_o) was calculated over periods of 60–500 s as follows. The closed current level (i_c) was taken as the mode of the distribution around closed events. This current was subtracted from the current of a given bin, and the difference was multiplied by the number of events in that bin. The sum of these products yields the open channel area of the histogram. nP_o is given by dividing the open channel area by the single-channel current, i_{sc}. That is,

$$nP_o = \frac{\sum_{\text{bins}} [\,(i_{\text{bin}} - i_c) \cdot (No.\ events_{\text{bin}})\,]}{i_{sc}}. \quad (1)$$

For kinetic analysis, currents were filtered at a corner frequency (f_c) of 2 kHz and sampled at 5,000 s^{-1}. An event (transition) was counted each time a data point crossed the 50% level of the unitary channel current. For our recording system, the patch-clamp has a 5-kHz step response, a 5-kHz tape bandwidth, and a 2-kHz eight-pole Bessel filter, yielding an effective bandwidth (−3 dB point, f_{ceff}) of 1.74 kHz. With these settings, the "dead time" of the recording system is given by Colquhoun and Sigworth (1983), $T_{dead} = 0.179/f_{ceff}$. The "50% delay time" of the Bessel filter is $T_{50\%} = 0.506/f_c$. For $f_{ceff} = 1.74$ kHz and $f_c = 2$ kHz, $T_{dead} = 102.8$ μs and $T_{50\%} = 253$ μs. Therefore, events in time histogram bins <500 s were cut off. Since an event lasting 253 μs would be the margin of detection, all dwell lifetimes <253 μs would be missed events.

Open and closed dwell-time kinetics were fit to a probability density function expressed as a sum of exponentials,

$$f(t) = \sum_{i=1}^{n} \frac{A_i}{\tau_i} \cdot e^{-t/\tau_i}, \quad (2)$$

where n is the number of open or closed states, the A_i are the relative amplitudes, and the i are time constants. This function was transformed according to $x = \ln(t)$ and logarithmically binned (Sigworth and Sine, 1987), such that

$$f(x) = \sum_{i=1}^{n} A_i \cdot e^{\{(x-x_i) - e^{(x-x_i)}\}}. \quad (3)$$

This function was used to fit the data using the Levenberg-Marquardt nonlinear least-squares fitting algorithm (Origin 4.0; Microcal Software, Inc., Northampton, MA) to find the appropriate set of τ's. Note that if the errors follow a Gaussian distribution, this nonlinear least-squares method is equivalent to the method of maximum likelihood (Colquhoun and Sigworth, 1983).

Dose–response relations for a drug (D) were fitted to the Hill equation as

$$\frac{I}{I_{\max}} = \left[1 + \left(\frac{K_i}{[D]}\right)^{n_H}\right]^{-1}, \quad (4)$$

where I/I_{max} is the fractional inhibition, K_i is the concentration of drug giving 50% inhibition, $[D]$ is the concentration of the drug, and n_H is the Hill coefficient. When $n_H = 1$, this equation reduces to the Langmuir adsorption isotherm.

In the text, the number of observations or experiments is reported, whereas n in the analysis denotes either the whole data set or the subset of total experiments in which precise quantitation could be reliably applied. In some figures, a running average (using a specified window width) of current versus time is displayed. Statistical values for the n elements are given as mean ± SEM. Student's t test was applied where appropriate.

RESULTS

Properties of the BLM K^+ Channel

Overview. With $[K^+] = 95$ mM in the patch pipette, we found the K^+ channel in 551 of 559 seals made on the BLM (98.6%). This K^+ channel was never detected in seals made on the apical membrane (0 of 16, 0%), consistent with our previous finding that dissociated *Ambystoma* proximal tubule cells retain epithelial cell polarity (Segal et al., 1996). Seals on the BLM typically contained from 2 to >25 K^+ channels. Despite numerous attempts to minimize patch area using small-tipped pipettes (resistance ≥ 30 MΩ), patches appearing to have one and only one channel were very infrequent ($n = 4$, only 0.7%).

Cell-attached patches. When cell-attached (c/a) patches were made in NaCl bath, spontaneous inward K^+ currents were usually observed (95%) at 0 mV ($-V_{pip}$) command potential. By briefly switching to zero current clamp mode, the resting membrane potential (V_m) of the cell can sometimes be estimated if $R_{seal} >> R_{patch}$. Using this method under these conditions, V_m averaged −37.2 ± 2.1 mV ($n = 16$), in good agreement with $V_m = -40$ mV as measured by conventional impalement (Segal et al., 1996). The V_m of the dissociated cells is ~15–20 mV less than that for a cell in the intact tubule (Sackin and Boulpaep, 1983), suggesting an anion conductance exists at either the apical or basolateral membrane. Indeed, we have characterized a cAMP-activated Cl^- channel in the BLM of these cells, which often appears in the same membrane patch as the K^+ channel (not shown). Alternatively, the isolated cells may have acquired a nonspecific leak pathway that shunts the normally high K diffusion potential. Since the K^+ and Cl^- activity of the pipette solution ($aP_K = 0.80*[95] = 76$ mM and $aP_{Cl} = 0.78*[92] = 71.8$ mM) is greater than the intracellular K^+ and Cl^- activity ($a^i_K = 0.80*[68] = 54.4$ mM and $a^i_{Cl} = 0.78*[20.5] = 16$ mM (Sackin and Boulpaep, 1983), yielding a reversal potential (E_{rev}) of −28.7 mV. Thus, at $-V_{pip} = 0$ mV, the inward current must be carried by K^+ moving down its electrochemical gradient from the pipette into the cell.

Representative c/a current records at various command potentials are shown in Fig. 2 *A*, and the current–voltage (I-V) characteristic is shown in Fig. 2 *B*. The inward slope conductance is 22.2 ± 1.4 pS (taken from −40 to −80 mV, $n = 8$), and the outward slope conductance (from +20 to +80 mV) is 3.5 ± 0.1 pS ($n = 5$), and channel activity appears to increase with hyperpolarization (Fig. 2 *A*). Although the c/a I-V char-

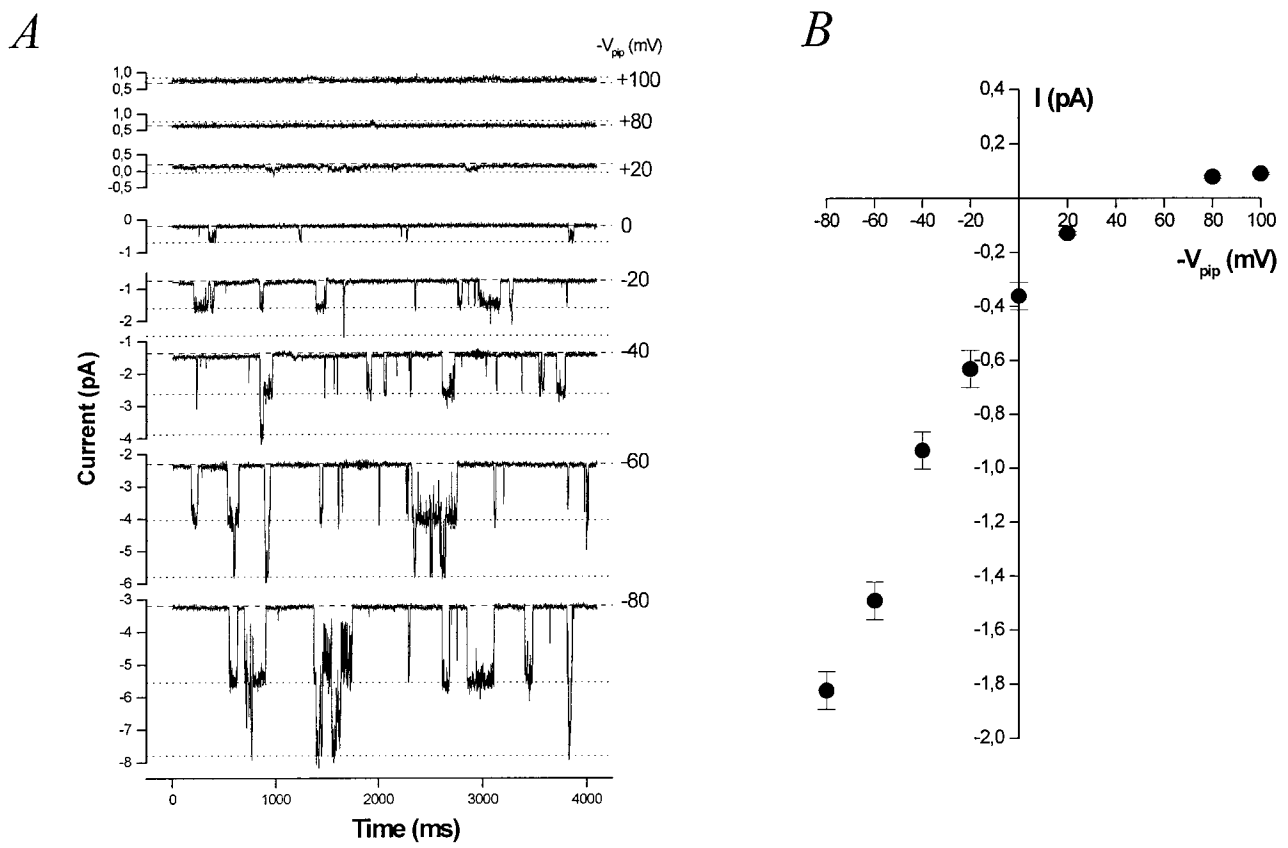

FIGURE 2. The BLM K^+ channel appears to be an inward rectifier. (*A*) Representative current records at various command potentials ($-V_{pip}$) from a cell-attached basolateral membrane patch containing at least two K^+ channels. Note the increase in channel activity with hyperpolarization. The patch pipette contains 95 mM K^+ (solution *d*) and the bath is NaCl (solution *c*). The dashed line represents the all channels closed (leak) current at each potential. Each open channel level is denoted by a dotted line. (*B*) Current–voltage relation for the BLM K^+ channel for the conditions described in *A*. The limiting inward slope conductance is 22.2 ± 1.4 pS (n = 8) and the outward chord conductance 3.5 ± 0.1 pS (between 120 and 180 mV, $n = 5$). Symbols represent mean (●) ± SEM (*bars*).

acteristic displays inward rectification, suggesting that the channel is an inward rectifier; under these conditions, the I-V relation would be expected to "inwardly rectify" due to Goldman-Hodgkin-Katz rectification.

Excised patches. When BLM membrane patches were excised in the inside-out (i/o) configuration into the standard bath solutions (solution *c* or *d*), channel activity typically began to decline and then disappear. Addition of 0.2 mM ATP to the bath before or just after patch excision prevented rundown and maintained channel activity indefinitely.

Measurements of single-channel current with $[K^+]$ = 95 mM on both sides of the membrane patch (plus 0.2 mM ATP on the cytosolic side) demonstrate that the BLM K^+ channel is a true inward rectifier (Fig. 3, *A* and *B*). The I-V relation in symmetrical $[K^+]$ inwardly rectifies and reverses very close to $E_K = 0$ mV. The channel has an inward slope conductance of $\gamma_{slope,\ in} = 24.5 \pm 0.6$ pS ($n = 8$, measured between −60 and −100 mV), and an inward chord conductance of $\gamma_{chord,\ in} = 20.5 \pm 0.4$ pS ($n = 8$, measured between $E_{rev} = 0$ and −100 mV). The outward chord conductance measured at +80 mV is $\gamma_{chord,\ out} = 3.7 \pm 0.4$ pS ($n = 2$). The outward slope conductance between +20 and +80 mV is clearly smaller.

Voltage dependence of nP_o. Since BLM membrane patches almost always contained more than one K^+ channel, nP_o (channel activity) was used to assess the relative voltage dependence of P_o. This assumes that the number of active channel proteins in an excised patch remains constant as voltage varies. (We take n as the maximum number of simultaneously open channels observed, which places a minimum on the actual number of channel proteins in the patch.) As was the case for cell-attached patches, channel activity with KCl on both sides of the excised membrane patch increases with increasing hyperpolarization (Fig. 3 *C*). Although the absolute values of nP_o differed significantly among patches, relative nP_o increased e-fold per ~83-mV hyperpolarization between −40 and −120 mV, reflecting a 27% increase of nP_o for every 20 mV of hyperpolarization.

Role of magnesium. It has been shown that $[Mg^{2+}]_i$ mediates at least part of the inward rectification in other inwardly rectifying K^+ channels (Matsuda et al.,

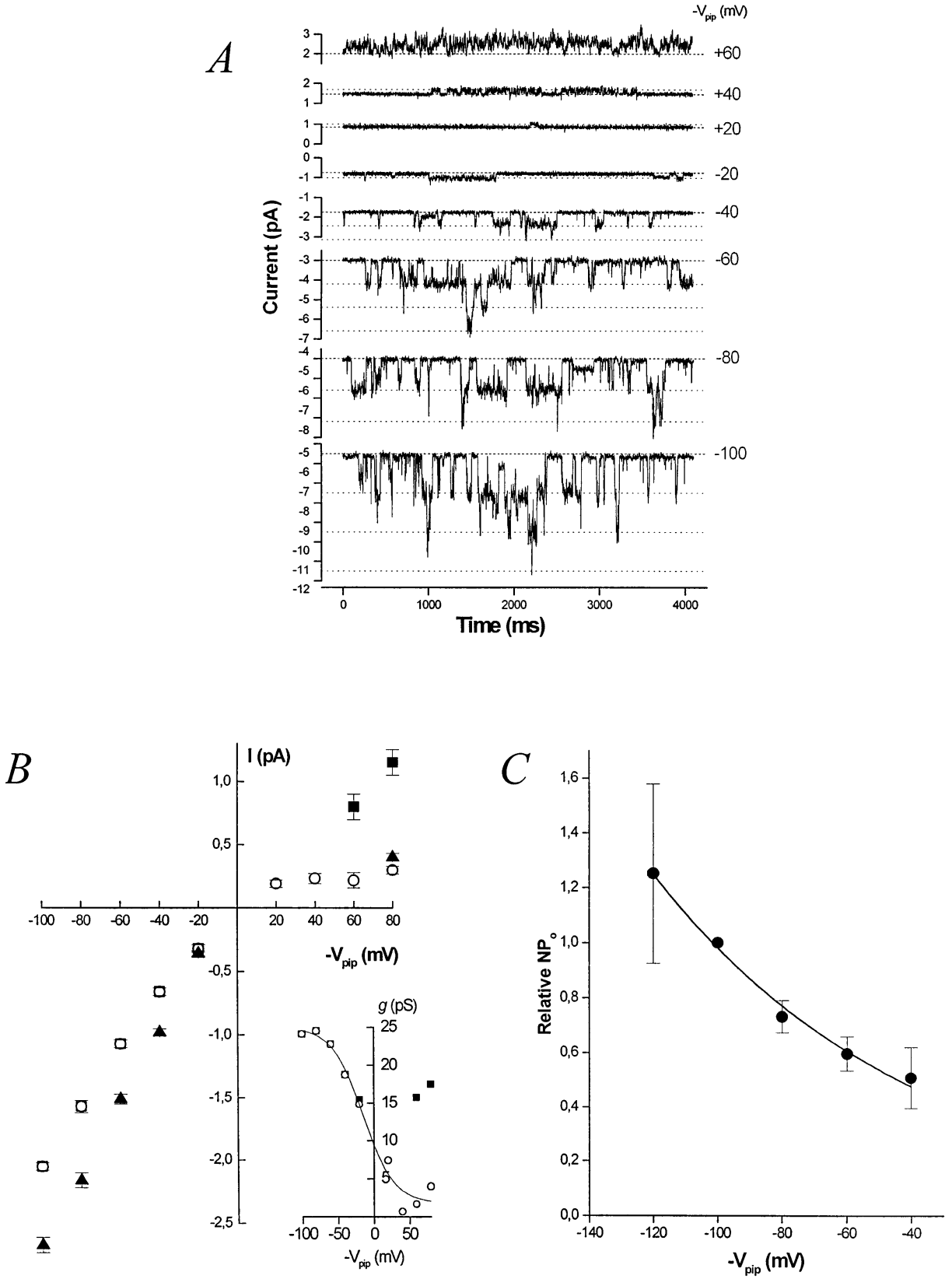

FIGURE 3. The BLM K^+ channel is a true inward rectifier. Representative current records at various command potentials ($-V_{pip}$) from an inside-out basolateral membrane patch in symmetrical [K] containing at least three K^+ channels. The patch pipette and bath each contain 95 mM K^+ (solution *d*) with 0.2 mM ATP added to the bath. The dashed line represents the all channels closed (leak) current at each po-

1987; Horie et al., 1987; Ficker et al., 1994) by blocking outward currents in a voltage-dependent manner. When Mg^{2+}_i was removed from the "cytosolic" side of i/o patches (solution *e* plus 0.2 mM Na_2ATP), we observed flickering, and then rundown of the channel. This is in sharp contrast to the behavior of ROMK1 channels, in which channel rundown is slowed in a Mg^{2+}-free bath (McNicholas et al., 1994). Since rundown occurs in the absence of free Mg^{2+}_i and the presence of 0.2 mM Na_2ATP ($n = 4$), it appears that at least the complex of Mg-ATP is required to prevent rundown. Interestingly, it has been shown that both Mg-ATP and free Mg^{2+}_i are required to sustain channel activity for an ATP-insensitive inward rectifier K^+ channel (Fakler et al., 1994). However, since higher levels of ATP block the BLM K^+ channel (see below), it is not possible for us to dissociate the role of free Mg^{2+}_i from that of the Mg-ATP complex. Millimolar concentrations of ATP (or indeed, any nucleotide) block the BLM K^+ channel, and this effect is independent of both free Mg^{2+}_i and Mg-ATP.

In a solution containing 368 nM Mg-ATP and 200 nM free $[Mg^{2+}]_i$ (solution *f*) (Fabiato and Fabiato, 1979), channel rundown did not occur. Although Fakler et al. (1994) showed that >10 μM free $[Mg^{2+}]_i$ is required to prevent rundown from occurring in the $K_{ir}2.1$ channel, just 200 nM free $[Mg^{2+}]_i$ is sufficient for the BLM K^+ channel. Under this condition, the outward unitary conductance of the latter increases, but the inward conductance is essentially unaffected. The enhanced outward current is ATP sensitive, as 5 mM ATP blocked 89.3 ± 6.3% ($n = 3$) of the current. The outward chord conductance with $[Mg^{2+}]_i$ = 200 nM increased from 4.25 ± 0.59 pS to 14.4 ± 1.2 pS ($n = 4$, measured at +80 mV); inward currents were not affected by the change in $[Mg^{2+}]_i$ (Fig. 3 *B*). Inward rectification was reestablished by returning bath $[Mg^{2+}]_i$ to 1 mM.

Assuming a single-binding site, the Mg^{2+} block may be described using a one-site model according to Woodhull (1973):

$$K(V_c) = K(0\,mV) \cdot \exp(-\delta V_c zF/RT), \qquad (5)$$

where V_c is the command potential, z is the valence of 2, and $K(V_c)$ and K(0 mV) are the concentrations of Mg^{2+} causing half-maximal block at V_c and 0 mV, respectively. The factor δ may be the electrical distance of the binding site from the outside of the channel pore. Alternatively, δ can be considered together with another term to yield either the equivalent valence (z) of, or the effective potential (V_c) sensed by, the Mg^{2+} (Hille, 1992).

Current–voltage relations from inside-out patches in symmetrical K^+ for several $[Mg^{2+}]_i$ were constructed, from which the current was normalized to that observed in a Mg^{2+}-free bath, and the relative current was plotted against command potential for each $[Mg^{2+}]_i$ (not shown). These data were then fitted (nonlinear least squares fitting routine) by the following function that incorporates Eq. 5:

$$\frac{I_{Mg^{2+}}}{I_{Mg^{2+}free}} = \frac{K(V_c)}{K(V_c) + [Mg^{2+}]}. \qquad (6)$$

The fit according to Eq. 6 yields the following results: δ = 0.57, K(0 mV) = 7.7 mM, K(60 mV) = 0.72 mM.

Concentration and voltage dependence of i_{sc}. To further investigate the biophysical properties of this channel, we asked the question of how varying extracellular $[K^+]$ would affect the current carried by the channel. To isolate the change in $[K^+]$ from any change in driving force across the patch, the same [KCl] was used in the pipette and bath, thus clamping E_{rev} to 0 mV. This approach allowed us to measure the change in absolute conductance while maintaining a constant relative permeability (i.e., we varied the Goldman-Hodgkin-Katz current equation while holding the result of the Goldman-Hodgkin-Katz voltage equation constant). Under these conditions, the command potential is the only driving force for net K^+ movement across the membrane patch. Pipette and bath [KCl] ranged from 5 to 205 mM while osmolality was kept at 400 mosm/kg using sucrose as necessary. Since i_{sc} for [KCl] = 95 mM was the same in both standard KCl solution (solution *d*, 200 mosm/kg) or 400 mosm/kg KCl solution, the tonicity change itself does not significantly alter the conducting properties of the channel.

Channel events (inward current) were analyzed at command potentials of −20, −40, −60, −80, and −100 mV for $[K^+]$ = 5, 10, 20, 25, 55, 95, 155, and 205 mM, and the I-V relationship was determined for each of these KCl concentrations. Channel events for $[K^+]$ = 5 mM could not be adequately resolved and were not included in the further analysis. For each voltage, the

tential. Each open channel level is denoted by a dotted line. (*B*) Effect of $[Mg^{2+}]_i$ on the I-V relation of the BLM K^+ channel. The inward rectification evident in 1 mM $[Mg^{2+}]_i$ (○) is relieved when $[Mg^{2+}]_i$ is lowered to 200 nM (■). (*inset*) Slope conductance–voltage (g-V) relation for the BLM K^+ channel in 1 mM $[Mg^{2+}]_i$ (○) and 200 nM $[Mg^{2+}]_i$ (■). Symbols represent mean ± SEM. The K^+ channel prefers Tl^+ over K^+. The I-V relation from inside-out patches with Tl-acetate (solution *g*) in the pipette and K-acetate (solution *h*) in the bath is also shown (▲). The limiting inward slope conductance is 29.0 ± 1.0 pS ($n = 4$) for Tl^+ compared with 24.5 ± 0.6 pS ($n = 8$) for K^+. (*C*) Channel activity (nP_o) increases with hyperpolarization. Data from four inside-out membrane patches in symmetrical [K] are plotted. Channel activity at command potentials of −120, −100, −80, −60, and −40 mV was normalized to that at −100 mV for comparison. Solid line is a single exponential fit with a voltage constant of ~83 mV. Symbols represent mean (●) ± SEM (*bars*).

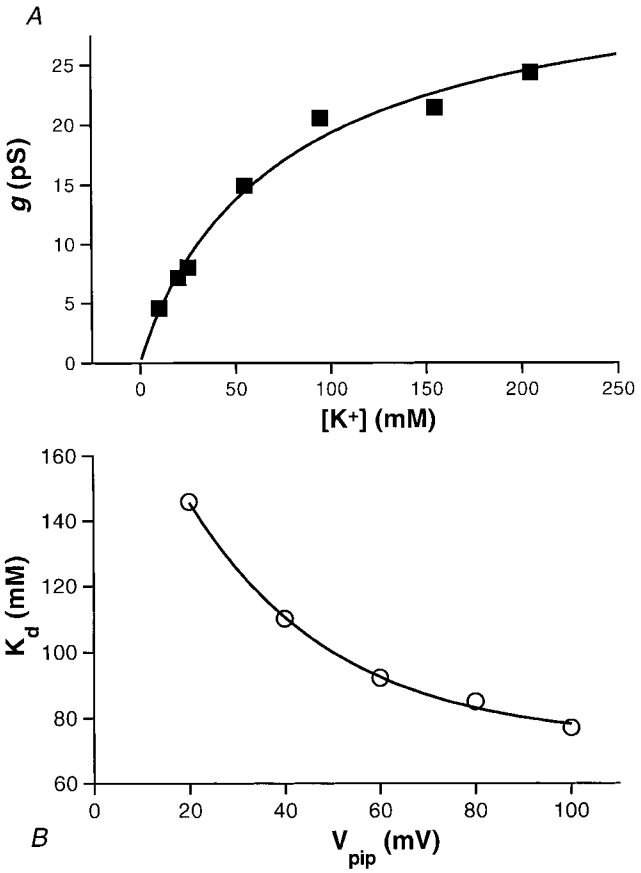

FIGURE 4. The operating surface of the BLM K^+ channel. (*A*) The single channel conductance (γ) at a command potential of −100 mV plotted as a function of $[K^+]$ and fit to the Hill equation according to $\gamma = \gamma_{max} \cdot [1 + (K_d/[K^+]_o)^{n_H}]^{-1} \cdot \gamma_{max}$ is the maximal value of the conductance, K_d is the apparent dissociation constant, and n_H is the Hill coefficient. For the chord conductance at −100 mV (■) and its least-squares fit (*solid line*), $\gamma_{max,slope}$ = 34.3 pS, K_d = 77 mM, and n_H = 0.94. (*B*) The plot of K_d versus V_{pip} shows that the apparent binding–unbinding rate of K^+ to the channel is voltage dependent. The data (○) were fit with a single exponential (*solid line*) as follows: $K_d = 73 + 141 \cdot \exp(-V_{pip}/30)$.

single channel current increases with $[K^+]$ and approaches a limiting current ($i_{max,sc}$). Similarly, the single channel chord conductance (γ_{chord}) also increases with $[K^+]$ and saturates (as shown for −100 mV in Fig. 4 *A*). Fitting the γ_{chord} versus $[K^+]$ data at −100 mV with the Hill equation:

$$\gamma = \gamma_{max} \cdot [1 + (K_d/[K^+]_o)^{n_H}]^{-1} \quad (7)$$

yielded a K_d of 77 mM, a Hill coefficient of 0.95, and a maximum value for γ_{chord} (γ_{max}) of 36.6 pS (Fig. 4 *A*). Plots of γ_{chord} versus $[K^+]$ at different voltages yielded similar results for γ_{max}. The average value for γ_{max} determined at −60, −80, and −100 mV was 34.3 pS. $\gamma_{max,sc}$ was the same for all command potentials fitted. Indeed, the intersection of the channel's operating surface with the I-V plane as K shows a linear conductance. This mean value for γ_{max} was applied to obtain K_d values and Hill coefficients for all the voltages (Table II).

TABLE II

K_d Values and Hill Coefficients for the BLM K^+ Channel

Command potential	K_d	Hill coefficient
mV	*mM*	n_H
−20	146	0.94
−40	110	1.02
−60	92	0.96
−80	85	1.00
−100	77	0.95

Comparison of the dissociation constants K_d for the different command potentials shows that K_d decreases with hyperpolarization (Fig. 4 *B* and Table II). The relationship between K_d (mM) and voltage (mV) can be described by a single exponential decay

$$\begin{aligned} K_d(V) &= K_{d,\infty} + K_{d,0} \cdot \exp\left(-\frac{V}{\psi}\right) \\ &= 73 + 141 \cdot \exp\left(-\frac{V}{30}\right) \end{aligned} \quad (8)$$

where $K_{d,}$ is the asymptotic value for K_d as $V_{pip} \rightarrow \infty$, $K_{d,0}$ is the difference of K_d at the reversal potential (0 mV) and $K_{d,\infty}$. Finally, ψ is the voltage change required to effect an e-fold change in $(K_d - K_{d,\infty})$.

Cation selectivity. The cation to anion preference of the total BLM conductance was determined by salt dilution experiments using i/o membrane patches. Starting in symmetrical 95 mM K^+ and 94.5 mM Cl^- ($E_K = E_{Cl} = 0$ mV) and holding at $-V_{pip} = 0$ mV, the bath was changed to a 14 mM K^+ and 13.5 mM Cl^- solution (solution *i*, $E_K = +48.6$ mV, $E_{Cl} = -49.4$ mV) plus sucrose to maintain isoosmolality. This maneuver resulted in large inward currents ($n = 3$), reflecting the cation (K^+) moving down its chemical gradient. The reversal potential for this membrane current (including leak) was at least +40 mV ($n = 3$). While holding at this E_{rev}, outward current developed when the 10% KCl bath was replaced with 100% KCl, due to K^+ moving along its electrical gradient. Thus, the BLM conductance is cation selective.

Using the Goldman-Hodgkin-Katz voltage equation (Hodgkin and Katz, 1949; Goldman, 1943) for K^+ and Cl^-, the permeability ratio p_K:p_{Cl} can be estimated (see MATERIALS AND METHODS):

$$E_{rev} = \frac{RT}{F} \ln \frac{p_K [K]_o + p_{Cl} [Cl]_i}{p_K [K]_i + p_{Cl} [Cl]_o}$$

$$\Leftrightarrow \frac{p_K}{p_{Cl}} = \frac{\exp\left(\frac{E_{rev}}{RT/F}\right) \cdot [Cl]_o - [Cl]_i}{[K]_o - \exp\left(\frac{E_{rev}}{RT/F}\right) \cdot [K]_i}. \quad (9)$$

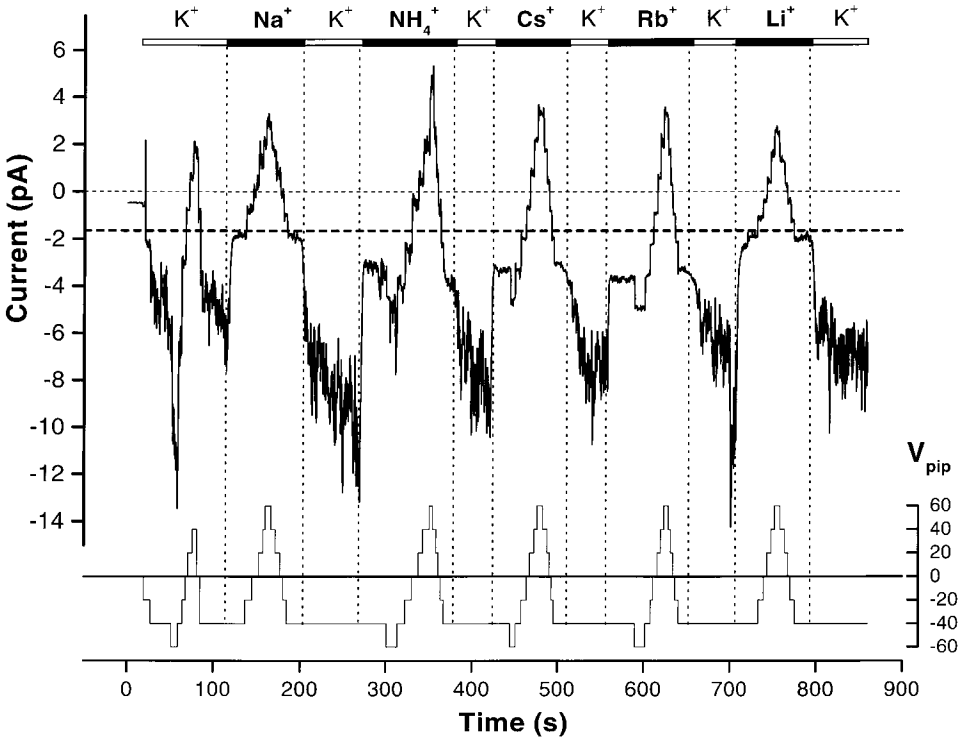

FIGURE 5. The BLM K^+ conductance is highly selective for K^+. The cationic selectivity of the BLM is demonstrated in this outside-out patch with KCl (solution *d*) + 0.2 mM ATP in the pipette and Cl-salt of the test cation in the bath. The running average of current at −40 mV shows that cationic selectivity is $K^+ >> Rb^+ \approx Cs^+ \approx NH_4^+ > Na^+ \approx Li^+$. The dashed line is the zero-current line, and the dotted line is the all channels closed (leak) current at a command potential of −40 mV. The voltage protocol is indicated below the current data.

where $R = 8.315$ J K^{-1} mol^{-1}, $F = 9.648 \cdot 10^4$ C mol^{-1}, $T = 293$ K, $E_{rev} \geq +40$ mV, $[Cl]_o = 94.5$ mM, $[K]_o = 95$ mM, $[Cl]_i = 13.5$ mM, and $[K]_i = 14$ mM, yielding p_K: p_{Cl} of at least 17:1. Note that even a small change in E_{rev} to +44 mV would double the selectivity ratio. It is emphasized that this value represents the minimum cation to anion preference of the K^+ channel since this is the selectivity ratio of the whole basolateral membrane patch including chloride and leak conductances.

Selectivity among cations. Two approaches were used to determine the selectivity of this inwardly rectifying K^+ conductance on the BLM. (*a*) Using c/a and i/o patches, the K^+ in the patch pipette was replaced with the chloride salt of Na^+ ($n = 48$), Rb^+ ($n = 4$), Li^+ ($n = 4$), Cs^+ ($n = 2$), or NH_4^+ ($n = 7$). Each solution was adjusted to pH 7.5 with the respective hydroxide salt. In all cases, c/a and i/o patches failed to show inward channel currents. These results strongly suggest that the BLM K^+ channel is highly selective for K^+ and excludes these cations, since channel activity is seen in >98% of seals made on the BLM when K^+ is in the pipette. (*b*) Outside-out patches were made to exclude the remote possibility that the c/a and i/o patches used above did not contain any channels. The pipette was filled with KCl, and 0.2 mM Mg-ATP was included to prevent channel rundown. After recording in a KCl bath, the test cation was introduced into the bath (as the chloride salt) and the voltage protocol was repeated. KCl bath exchanges were interposed between test cations.

The cation selectivity as determined from outside-out patches is exemplified in Fig. 5. For Na^+ and Li^+, the current at −40 mV is negligible, but a modest inward current is carried by Rb^+, Cs^+, and NH_4^+. Exchanging the test cation with KCl returned the ensemble currents to the control level in all cases. That the outward current carried by K^+ remains essentially unchanged during each bath cation substitution indicates that the test cations do not act as channel blockers from the outside. The ensemble current obtained at $V_{pip} = -40$ mV shows that the selectivity of the channel for these cations is $K^+ >> Rb^+ \approx Cs^+ \approx NH_4^+ > Na^+ \approx Li^+$.

Thallium. Many types of K^+ channels have been shown not only to conduct Tl^+, but often better than they conduct K^+ (Hille, 1992). To assess the Tl^+ conductance of the BLM K^+ channel, the patch pipette was filled with 90 mM Tl-acetate (solution *g*; the Cl salt of Tl^+ was not used due to its low aqueous permeability) and the bath was filled with K-acetate (solution *h*). Under these conditions, inward Tl^+ currents were observed in both c/a and i/o patches. The kinetic behavior of these channel events was notably different from those seen when the channel conducts K^+. When conducting Tl^+, the channel openings displayed more bursting, with each opening interrupted by fast flickery closures. The probability that this is actually a different channel is low since (*a*) the frequency of finding the K^+ channel exceeds 98%, (*b*) other cation-selective channels were rarely observed, (*c*) the disparate kinetics

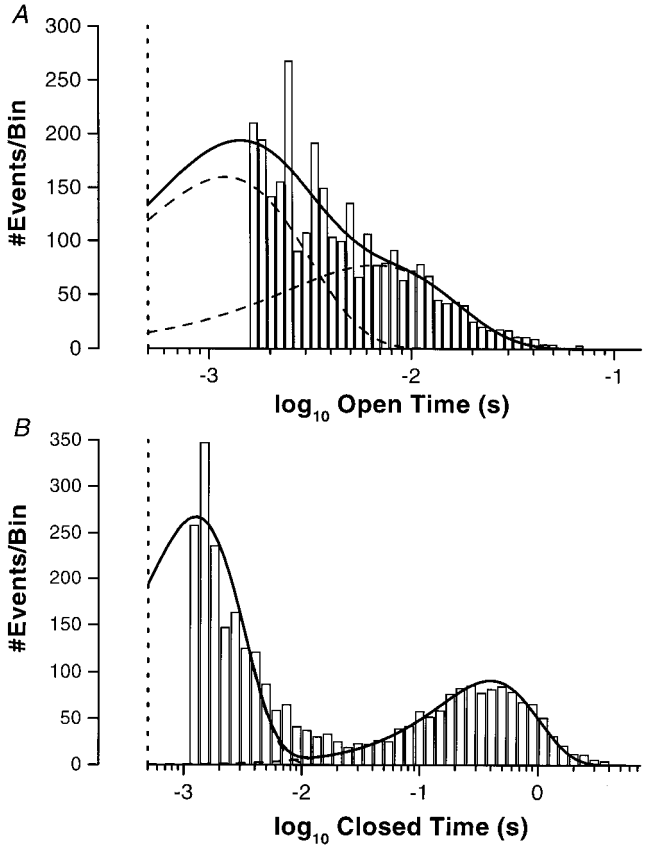

FIGURE 6. Kinetics of the BLM K^+ channel. (*A*) Open-time histogram for the BLM K^+ channel in a cell-attached patch at −60 mV with the time intervals logarithmically binned (Sigworth and Sine, 1987). The data were fitted with two probability density functions (*dashed lines*) to give the overall fit (*solid line*), yielding time constants of τ_{o1} = 0.78 ms (78%) and τ_{o2} = 4.7 ms (22%). Based on the bandwidth of the recording system, the data and the fit were cutoff at 500 μs (*vertical dotted line*). (*B*) Closed-time histogram for the BLM K^+ channel in a cell-attached patch at −60 mV with the time intervals logarithmically binned. The data were fitted with two probability density functions (*dashed lines*) to give the overall fit (*solid line*), yielding time constants of τ_{c1} = 1.27 ms (74%) and τ_{c2} = 397 ms (26%). Based on the bandwidth of the recording system, the data and the fit were cutoff at 500 μs (*dotted vertical line*).

were only seen when Tl^+ was in the pipette, and (*d*) Tl^+ currents were sensitive to glibenclamide (see below).

The I-V relationship for this biionic condition is shown in Fig. 3 *B*. The limiting inward slope conductance for Tl^+ was 29.0 ± 1.0 pS (measured between −60 and −100 mV, n = 4). Thus the channel conductance is slightly higher for Tl^+ than it is for K^+ ($g^*_{in}Tl$: $g^*_{in}K$ = 1.2:1). Since small inward currents were observed while holding at 0 mV in two i/o experiments with Tl^+ in the pipette and K^+ in the bath, the reversal potential is positive. This implies that the permeability (zero-current conductance) for Tl^+ is also greater than that for K^+. Therefore, compared with K^+, Tl^+ has a higher conductance and is more permeant but probably interacts with the pore, causing a fast channel block.

In conclusion, these findings indicate that the permeability sequence of this K^+ channel is $Tl^+ > K^+ >> Cs^+ \approx Rb^+ \approx NH_4^+ > Li^+ \approx Na^+ > Cl^-$.

Kinetics. Due to the high density of this K^+ channel in the BLM, a patch apparently containing only one channel is extremely rare. In over 550 seals, only four membrane patches appeared to contain only one channel (0.7%). Since the open probability (P_o) of the channel is only 0.05 ± 0.01 (n = 4), long recordings were required to accumulate enough transitions for meaningful analysis of the long closed state. Kinetic analyses from such patches show that under resting state conditions at $-V_{pip} = -60$ mV, the BLM K^+ channel has two apparent open states and two apparent closed states. Parameters from one c/a patch and one i/o patch show that the open dwell lifetimes are (ms): τ_{o1} = 0.78 (c/a), 1.21 (i/o), and τ_{o2} = 4.7 (c/a), 6.6 (i/o). The closed dwell lifetimes are (ms): τ_{c1} = 1.27 (c/a), 0.72 (i/o), and τ_{c2} = 397 (c/a), 502 (i/o). Fig. 6 shows the open and closed time histograms for a c/a patch.

Inhibitor Profile

The BLM K^+ channel is inhibited by barium and glibenclamide. The channel is insensitive to tetraethylammonium (up to 10 mM) applied either to the extracellular or cytoplasmic side.

Barium. We have previously shown by recording single-cell membrane potential that the whole cell conductance is dominated by a barium-sensitive K^+ conductance (Segal et al., 1996). Perforated patch whole-cell recordings show that the barium-sensitive whole cell conductance inwardly rectifies. When 2 mM Ba^{2+} was included in the KCl pipette solution (unpaired experiments), channel openings were rare and a flickery state was noted. In contrast to the voltage dependence of channel activity without Ba^{2+} in the pipette (see Fig. 3 *C*), steady depolarization now has the effect of increasing nP_o, and subsequent hyperpolarization reduced activity. This is presumably due to the voltage dependence of the Ba^{2+} block of the channel (data not shown).

To quantify the Ba^{2+} block and use each patch as its own control, outside-out patches were made (n = 3). In outside-out membrane patches at −40 mV, Ba^{2+} inhibits the channel with a K_i = 460 μM (Fig. 7 *A*).

Glibenclamide. This sulfonylurea is known to inhibit ATP-sensitive K^+ channels in a number of epithelial tissues by binding to the sulfonylurea receptor (SUR). SUR1 has recently been cloned (Aguilar-Bryan et al., 1995) and is thought to associate with the K_{ATP} channel, thereby conferring sulfonylurea sensitivity. However, SUR1 may not be present in the kidney (Inagaki et al., 1995), which may explain in part the much higher dose of glibenclamide required to inhibit renal K_{ATP} channels (Hebert and Ho, 1994). In this context,

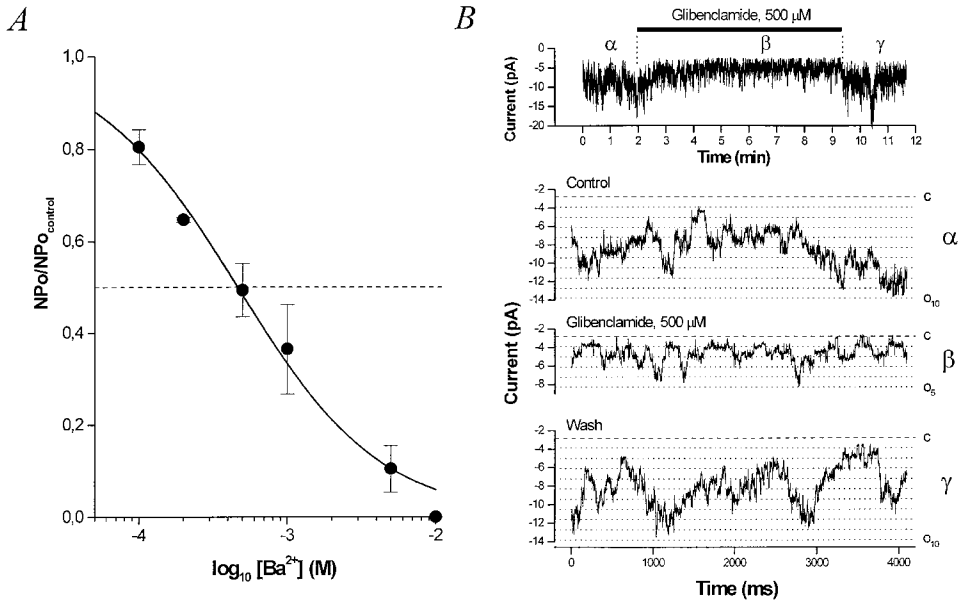

FIGURE 7. Inhibitors of the BLM K^+ channel. (*A*) Dose–response curve for inhibition of the BLM K^+ channel by external Ba^{2+}. Relative nP_o ($nP_o/nP_{o,control}$) determined from outside-out patches at a command potential of −40 mV with KCl in the pipette and bath (solution *d*) is plotted versus [Ba^{2+}]. The data at −40 mV were fitted with the Hill equation (*solid curve*), yielding a K_i = 460 μM and n_H = 0.90. The inhibition by Ba^{2+} is fully reversible. (*B*) Glibenclamide inhibits the BLM K_{ATP} channel. (*top*) A running average (window width 16 ms) of current versus time. Glibenclamide (500 μM) is added to the bath where indicated. (*bottom*) Sample traces from a representative experiment at −60 mV with KCl in the pipette and bath (solution *d*). Exposure of this inside-out patch to 500 μM glibenclamide reversibly decreases nP_o by ~50%. The dashed line denotes the all channels closed (leak) current level and the dotted lines indicate each open channel level.

the BLM K^+ channel is glibenclamide sensitive, albeit at "renal doses." We treated 22 patches with glibenclamide; 16 excised inside-out patches were exposed to 500 μM, while 6 cell-attached patches were exposed to low (0.01–10 μM) concentrations. In 7 of 16 inside-out patches, 500 μM glibenclamide inhibited activity by 42.3 ± 5.6% (Fig. 7 *B*). Remarkably, the inhibition was much more potent in the cell-attached patches: 10 μM exerted an 83 ± 2% inhibition in three patches, and 100 nM exerted a 70 ± 3% inhibition in three other patches (data not shown).

ATP Sensitivity

Similar to other K_{ATP} channels, low doses of ATP are required to prevent *Ambystoma* BLM K^+ channel rundown, whereas millimolar doses inhibit channel activity. At a dose of 5 mM ATP, >90% of channel activity is inhibited. This effect is reversible as nP_o returns to baseline when the bath [ATP] is returned to 0.2 mM (Fig. 8 *A*). The dose–response curve for ATP has a K_i ~ 2.4 mM (Fig. 8 *B*). The Hill coefficient of ~4 may suggest that the channel has a tetrameric structure, with each subunit possessing an ATP binding site. Thus, in the *Ambystoma* proximal tubule, the BLM K^+ channel that appears to be the major K^+ conductance of the cell is ATP sensitive.

Among the nucleoside diphosphates, ADP is less potent than ATP (ADP inhibits by 65.6 ± 8.1%, n = 4, P < 0.01), but more potent than CDP, GDP, IDP, TDP, or UDP (data not shown). This suggests that the putative nucleotide binding site(s) recognize NDPs as well as NTPs, and that nucleotide hydrolysis is probably not occurring at this site. Indeed, even nucleoside monophosphates have a moderate inhibitory effect, although nucleosides themselves are without effect. The relative potency of the adenosine nucleosides (at 5 mM) in inhibiting the BLM K_{ATP} channel is ATP (93.3 ± 1.9%) > ADP (65.6 ± 8.1%) > AMP (38.7 ± 3.7%) > adenosine (1 ± 2%) (Fig. 8 *C*, n = 3–9).

Other nucleotides. The effect of nucleotides was tested in excised i/o patches. All the NTPs tested reversibly inhibited BLM K^+ channel activity at a dose of 5 mM (ATP 93.3 ± 1.9%, n = 9; CTP 70.3 ± 10.0%, n = 5; GTP 62.3 ± 7.5%, n = 3; ITP 61.1 ± 0.8%, n = 2; TTP 53.7 ± 6.7%, n = 2; UTP 71.7 ± 5.7%, n = 2) (Fig. 8 *C*). These results suggest that each compound probably interacts with common cytoplasmic nucleotide binding site(s). Note that ATP is significantly more potent than the other nucleoside triphosphates (P < 0.02), but there is no significant difference among the nonadenosine nucleotides.

Rundown of the BLM K^+ Channel

One characteristic of K_{ATP} channels is "rundown," a gradual loss of activity when the membrane patch is deprived of cytosolic ATP (Findlay and Dunne, 1986). Typically, both Mg^{2+} and ATP are required to prevent rundown in K_{ATP} channels (Ashcroft and Ashcroft, 1990). Likewise, the BLM K^+ channel runs down in the absence of either Mg^{2+} or ATP (or both). Lower concentrations of ATP (100–200 μM) will prevent or "rescue" channel rundown. The experiment shown in Fig. 9 *A* summarizes the characteristics of BLM K^+ channel rundown. Channel activity typically begins to decrease

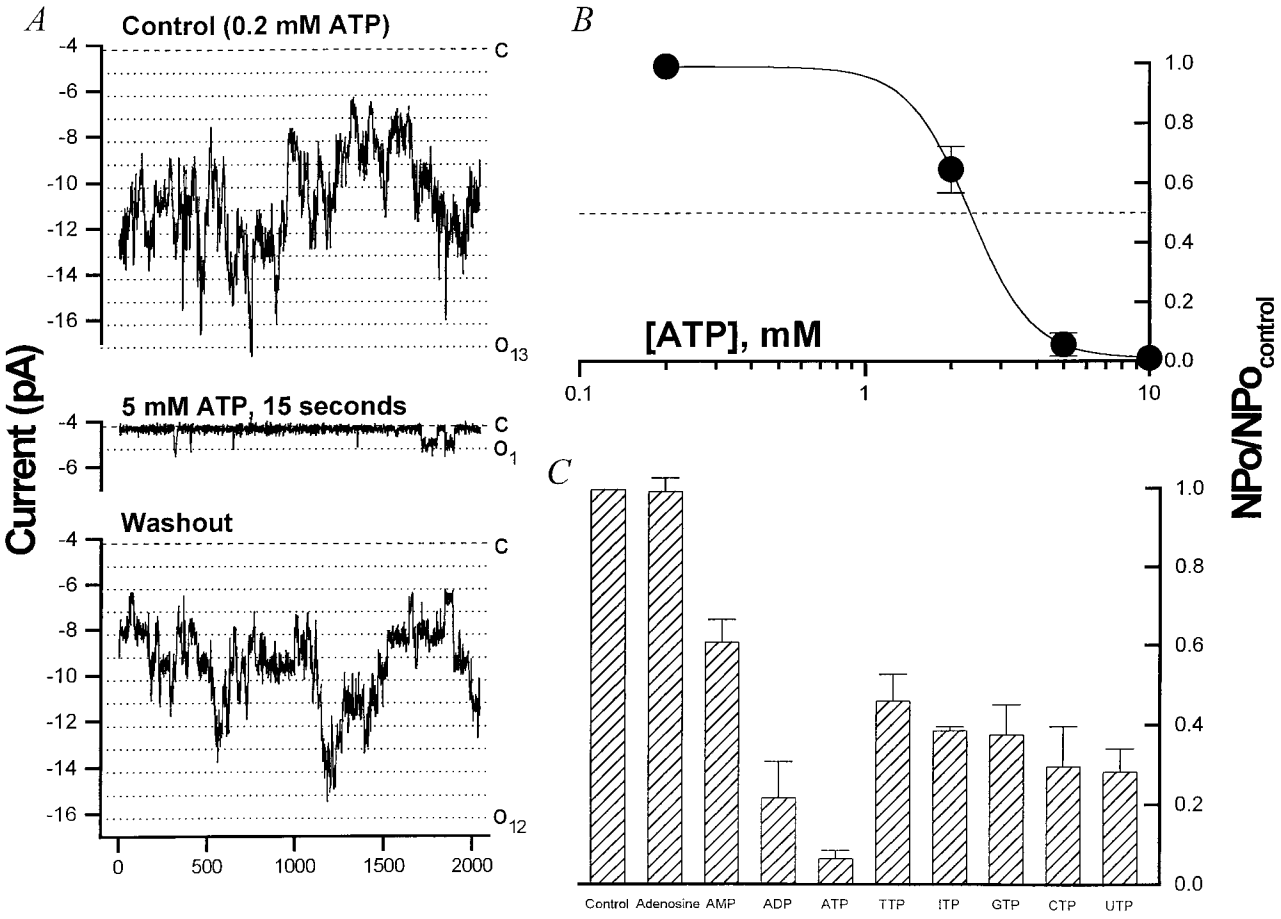

FIGURE 8. Nucleotides reversibly inhibit the BLM K^+ channel. (*A*) ATP_i reversibly inhibits the BLM K^+ channel in inside-out patches. In the experiment depicted, up to 13 channel open levels are seen under control conditions (*top*) at −60 mV with KCl (solution *d*) in the pipette and NaCl (solution *c*) plus 0.2 mM ATP in the bath. (*middle*) Addition of 5 mM ATP to the cytoplasmic side almost completely blocks channel activity (98% decrease) with only rare openings to one open level. (*bottom*) The inhibition is readily reversed upon returning to 0.2 mM ATP_i. (*B*) Dose–response curve for inhibition by ATP_i. The inhibitory effect of ATP_i was determined in inside-out patches under the conditions described in *A*. Relative nP_o ($nP_o/nP_{o,control}$) is plotted versus $[ATP]_i$. The data (●) was fitted with the Hill equation (*solid line*) yielding a $K_i \sim 2.4$ mM and $n_H = 3.95$. Adenosine nucleotides and nucleoside triphosphates (each at 5 mM) inhibit the BLM K^+ channel. The inhibitory effect of ATP, ADP, AMP, and adenosine was determined under the conditions described in *A*. Values plotted are average ($nP_{o,test}/nP_{o,control}$) SEM ($n$ = 3–9). The rank order of inhibition is ATP (93.3%) > ADP (65.6%) > AMP (38.7%). Adenosine has no inhibitory effect on nP_o of the BLM K^+ channel. Although all the nucleoside triphosphates inhibit the channel, ATP exerts a significantly stronger block than the other NTPs tested ($P < 0.02$). There is no significant difference among the other NTPs.

(rundown) upon excision of the membrane patch into a nucleotide-free bath. If this process is allowed to continue, channel activity will cease, usually irreversibly. When 0.2 mM of ATP is added back, channel activity can be restored. When ATP is removed, all channels rapidly close. In the continued presence of ATP-γS, readdition of ATP is again able to rescue rundown, and activity returns to baseline upon washout of the ATP-γS. Frequently (but not invariably), ATP-γS has an inhibitory effect on single channel activity when added in the presence of ATP, which is reversible as long as the exposure is not prolonged (n = 6), as shown in Fig. 9 *B*. When ATP-γS is added in the absence of ATP, channel activity runs down very quickly, usually irreversibly (n = 4, data not shown).

Thus, ATP-γS cannot substitute for ATP in sustaining channel activity, suggesting that phosphorylation itself is not sufficient to prevent rundown. Although phosphorylation may be necessary, it appears that the nucleoside triphosphate must be hydrolyzable to maintain channel activity. This hypothesis is supported by the finding that CTP, GTP, ITP, TTP, and UTP could all prevent or rescue rundown, but the corresponding NDPs could not. Rescue does not appear to require the cAMP-dependent protein kinase, since channel activity can be restored even in the presence of a high concentration of protein kinase inhibitor (PKI, 1 μg/ml, P-0300; Sigma Chemical Co.).

Since it has been reported that removal of free Mg^{2+} nearly abolishes rundown of K_{ATP} in cultured CRI-G1

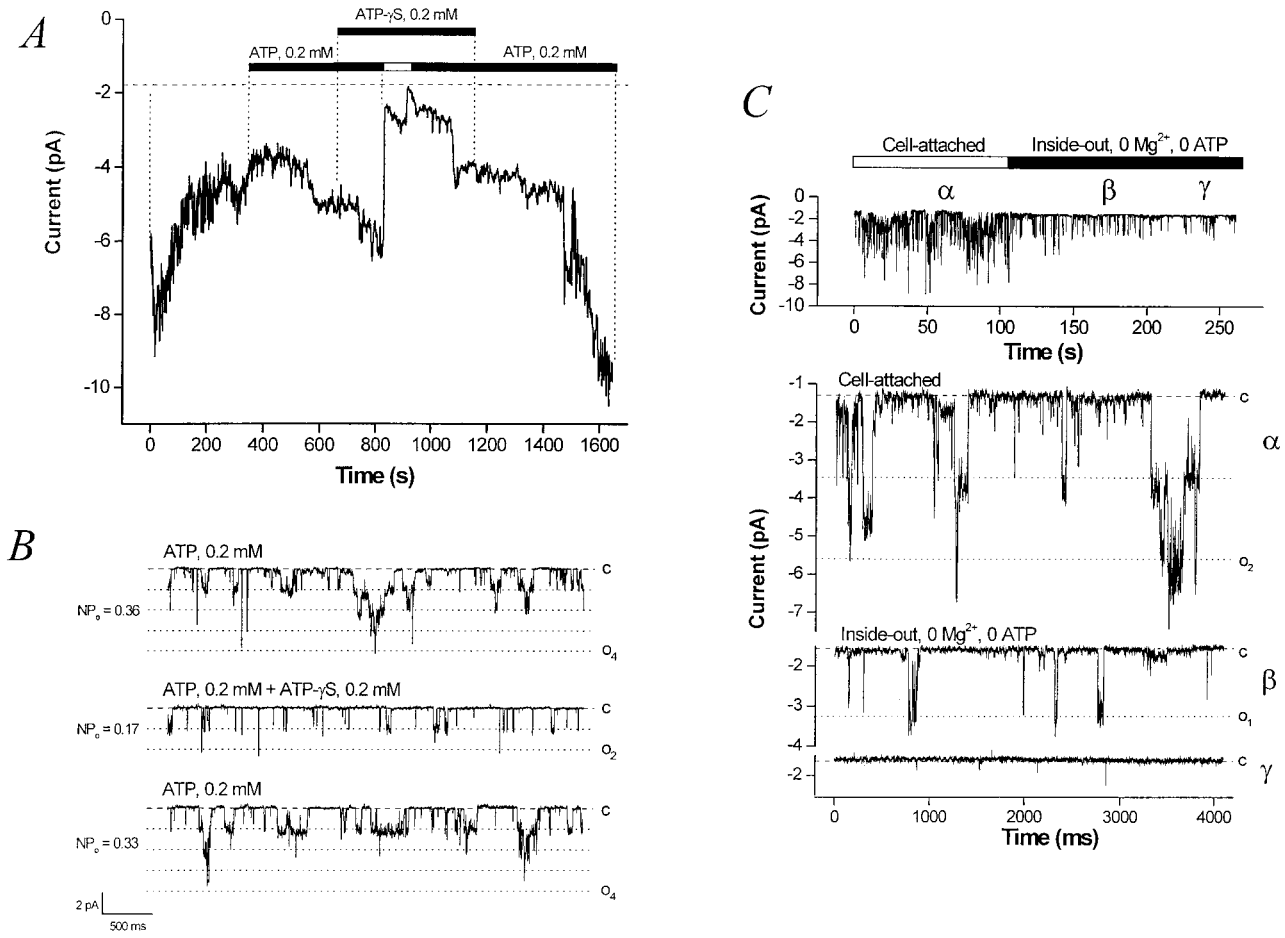

FIGURE 9. ATP but not ATP-γS prevents and rescues channel rundown. Hydrolyzable nucleoside triphosphates prevent and rescue BLM K^+ channel rundown. A running average (current versus time, window width 768 ms) of a representative experiment is shown. The pipette is KCl (solution *d*), the bath is NaCl (solution *c*), the command potential is −60 mV. Upon excision in a nucleotide-free bath, channel activity decreases (channel rundown). After the addition of 0.2 mM ATP to the bath, channel activity slowly recovers. The addition of 0.2 mM ATP-γS (a poorly hydrolyzable ATP analogue) in the continued presence of 0.2 mM ATP has no effect. However, when ATP is removed, ATP-γS is not able to support channel activity, which rapidly declines and runs down. Readdition of ATP leads to full recovery of channel activity. Single-channel traces showing that ATP-γS has an inhibitory effect on K_{ATP} channel activity in excised inside-out BLM patches. When compared with control conditions (*top*), the addition of ATP-γS (*middle*) reduces nP_o. This inhibition is reversible as long as the exposure to ATP-γS is not prolonged (*bottom*). (*C*) Removal of Mg^{2+} does not prevent channel rundown in an ATP-free bath. The top panel shows that rundown of the BLM K_{ATP} channel upon excision into an ATP-free bath proceeds despite removal of bath Mg^{2+}. Representative traces from the regions marked by α, β, and γ are shown at bottom.

insulin-secreting cells (Kozlowski and Ashford, 1990) and partially inhibits rundown of ATP-regulated ROMK1 channels excised in an ATP-free bath (McNicholas et al., 1994), we assessed BLM K_{ATP} channel activity under these conditions. The representative experiment shown in Fig. 9 *C* shows that rundown of the BLM K_{ATP} channel still occurs in the absence of ATP despite excision of the patch into a Mg^{2+}-free bath.

Diazoxide. The synthetic K_{ATP} channel opener diazoxide was applied to the cytoplasmic side of i/o patches. It has been shown that this benzothiadiazine can open K_{ATP} channels in the presence of Mg-ATP, but it may have an inhibitory effect in the absence of Mg-ATP (Kozlowski et al., 1989). Initial excision of the patch into an ATP-free bath leads to channel rundown as discussed above, and 200 μM diazoxide alone does not rescue rundown. However, addition of 0.2 mM Mg-ATP in the continued presence of, or after exposure to, diazoxide increases channel activity well in excess of that before rundown (n = 3, Fig. 10). The inhibitory effect of 5 mM ATP is not diminished in the presence of, or by previous exposure to, diazoxide (n = 5, data not shown).

Since low levels of Mg-ATP are required for diazoxide to open the BLM K^+ channel, diazoxide probably does not interact with the rundown site. As hypothesized by others (Edwards and Weston, 1993, 1995), diazoxide may be acting at or near the nucleotide binding

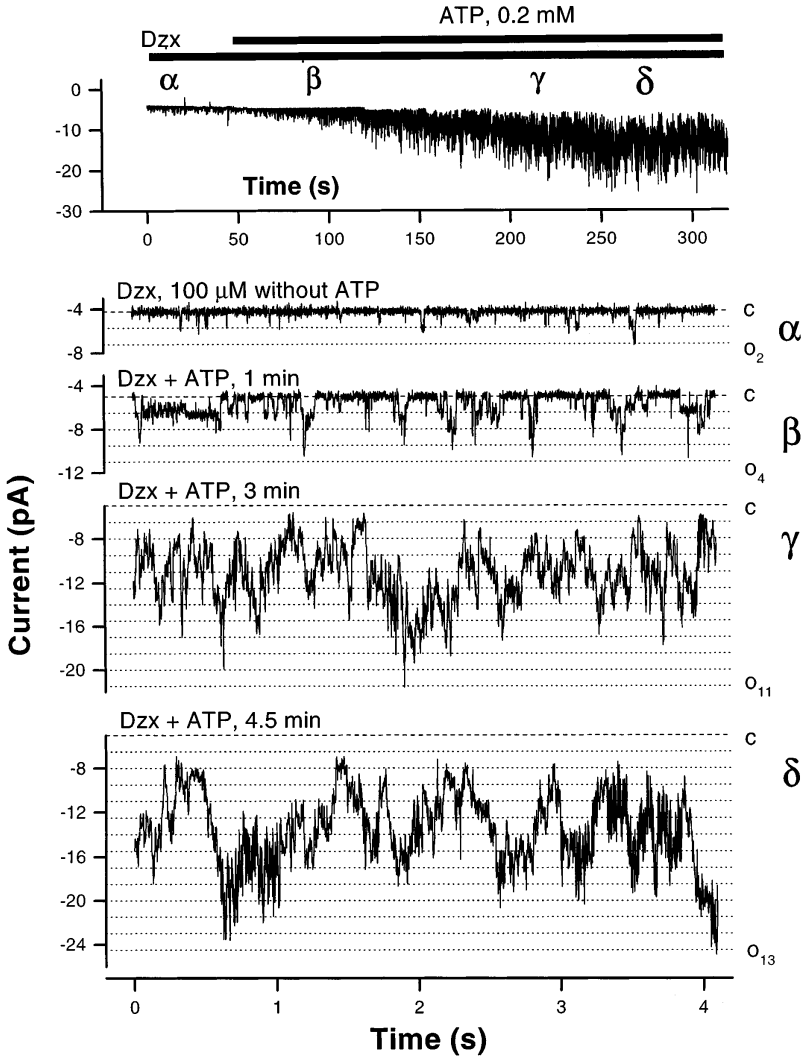

FIGURE 10. The K channel opener diazoxide activates the BLM K^+ channel. Diazoxide activates the BLM K^+ channel in the presence of ATP. In the experiment depicted, the pipette contains KCl (solution *d*), the bath contains NaCl (solution *c*), and the command potential is −80 mV. (*top*) A running average (window width 16 ms) of current versus time. (*bottom*) Sample current traces from the same experiment. With diazoxide alone, the channel opens infrequently (nP_o = 0.15) and no more than two channels are open at a time. Diazoxide combined with 0.2 mM ATP, however, promptly increases channel activity and within 5 min, up to 13 simultaneously open channels are evident (nP_o = 5.27). The all channels closed level (*dashed line*) and open channel levels (*dotted lines*) are indicated.

site that mediates inhibition. On the other hand, the interaction at this second site is more complex than a simple competition between the K channel opener and the nucleotide, since diazoxide does not relieve the inhibition by millimolar levels of ATP.

DISCUSSION

The proximal tubule (a leaky epithelium) can be considered to function within the general scheme of the epithelial transport model first proposed by Koefoed-Johnsen and Ussing (1958) (KJU), in which the apical membrane is primarily Na^+ selective and the BLM is primarily K^+ selective. Although this model was first applied to tight epithelia such as frog skin (Koefoed Johnsen and Ussing, 1958) and urinary bladder (Davis and Finn, 1982), its essence holds for leaky epithelia such as small intestine (Gunter-Smith et al., 1982) and the proximal tubule (Matsumura et al., 1984). In the KJU model, maintenance of unidirectional Na transport requires that K moves in a closed circuit (recycling) across the BLM. That is, barring intracellular accumulation of K (or K^+ secretion), the K^+ pumped into the cell by the pump must be matched by an outward K^+ current across the BLM.

Steady state vectorial transport in the proximal tubule thus requires continuous activity of the basolateral Na^+,K^+-ATPase pump, which consumes ATP and obligates intracellular accumulation of K^+. A conductance for K^+ is necessary both to allow this K^+ to recycle and to maintain V_{bl}. Experiments performed by Matsumura et al. (1984) on perfused *Necturus* proximal tubules first demonstrated that the BLM G_K varies as a function of pump activity, and they suggested that the regulation of BLM G_K was linked to cellular metabolism, as had been previously proposed for red cells (Romero, 1978) and suspensions of rabbit cortical tubules (Balaban et al., 1980).

This hypothesis was bolstered when the first single-channel records of an ATP-sensitive K^+ channel (K_i = 0.1 mM) from cardiac muscle were published (Noma, 1983). Similar ATP-sensitive K^+ (K_{ATP}) channels were

subsequently found in pancreatic β-islet cells (Cook and Hales, 1984), skeletal muscle (Spruce et al., 1985), and smooth muscle (Standen et al., 1989). The K_i for ATP is 10–100 μM for all these Type I K_{ATP} channels (Ashcroft and Ashcroft, 1990), and they are inhibited by sulfonylurea agents (Edwards and Weston, 1993). A K_{ATP} channel with these Type I properties has not been identified in epithelial tissues. However, a related K_{ATP} channel was recently demonstrated in nonperfused (Tsuchiya et al., 1992) and perfused (Hurst et al., 1993; Beck et al., 1993) rabbit proximal tubules. In preliminary experiments, we have also found this channel in the BLM of nonperfused rabbit proximal tubule, and in the present study we provide the first detailed description of the analogous BLM K_{ATP} channel in an amphibian using a novel preparation of dissociated proximal tubule cells that retain epithelial polarity (see Fig. 1 and Segal et al., 1996).

Investigators have used several techniques to patch the BLM, including mechanically stripping off the basement membrane (Sackin and Palmer, 1987; Kawahara et al., 1987) and tearing tubules to access the lateral membrane (Gögelein and Greger, 1987*b*). However, enzymatic treatment of nonperfused tubules (Tsuchiya et al., 1992; Parent et al., 1988), perfused tubules (Hurst et al., 1993; Beck et al., 1993), and single cells (Hunter, 1991) has been employed most commonly.

We have previously shown that the dissociated *Ambystoma* proximal tubule cells (see Fig. 1) retain epithelial cell polarity (Segal et al., 1996). Indeed, the K^+ channel described in the present study was present in >98% of seals made on the BLM, but was never detected in the apical membrane. With high [K] on both sides of the membrane patch, this BLM K^+ channel exhibits inward rectification with $\gamma_{slope,\,in} = 24.5 \pm 0.6$ pS and $\gamma_{chord,\,out} = 3.7 \pm 0.4$ pS. This non-ohmic behavior in both cell-attached and -free membrane patches is due at least in part to a voltage-dependent open channel block by cytosolic Mg^{2+} (Matsuda et al., 1987). Removal of Mg^{2+} from the cytosolic side of i/o patches leads to an increase in outward conductance without affecting inward conductance. In c/a patches made on frog BLM (NaCl pipette in a KCl bath), Hunter (1991) estimated that the blocking site was 51.3% across the membrane from the cytosolic side (i.e., 0.513). This compares well to the value of 0.57 obtained for the *Ambystoma* BLM K^+ channel in the present study.

Inward rectification of current is not necessarily due to a decrease in the intrinsic outward conductance of the channel pore. Indeed, Matsuda et al. (1987) first described how ohmic single channel units could behave as rectifiers. They showed that inward rectification of a cardiac myocyte K^+ channel was mediated by two effects: (*a*) Mg^{2+}-independent voltage gating in which ohmic channels are open at hyperpolarized voltages and essentially inactivate upon depolarization, and (*b*) a Mg^{2+}-induced voltage-dependent open channel (fast) block. Our data for the BLM K^+ channel are in keeping with these observations since (*a*) the conductance is ohmic in the absence of cytosolic Mg^{2+}, and (*b*) Mg^{2+} appears to cause a flickery open channel block of the outward current in the steady state (e.g., see Fig. 3 *A*). Naturally occurring polyamines (e.g., spermine) have also been shown to mediate inward rectification of some K^+ channels (Ficker et al., 1994). However, spermine (up to 5 mM) does not affect the *Ambystoma* BLM K^+ channel.

Properties of K^+ conduction through the pore. Constant-field theory predicts that net K^+ flux across the channel should increase linearly with rising $[K^+]$. Most channels do not exhibit this behavior due to "competition" for binding sites within the pore, and saturation occurs at higher concentrations of the permeant ion (Hille, 1992). In our study, conductance versus $[K^+]$ was fit with the Hill equation (Table II). Hill coefficients of ~1 suggest that one K^+ ion interacts with the channel at a time, allowing permeation to be modeled as follows:

$$K^+_{outside} + \text{channel} \underset{k_{-1}}{\overset{k_1}{\rightleftarrows}} [K^+ \text{bound to channel}]$$

$$\underset{k_{-2}}{\overset{k_2}{\rightleftarrows}} K^+_{inside} + \text{channel}.$$

At high $[K^+]$ concentrations, saturation occurs when the rate of ion entry approaches the maximum rate of unbinding. For the BLM K^+ channel, the maximum inward conductance ($\gamma_{max} = 34.3$ pS) is voltage-independent, suggesting that at high concentrations of K^+, the electrical driving force is the rate-limiting factor for ion flux. However, the binding-unbinding rate is voltage dependent, suggesting that the loading of the binding site for K^+ is dependent on the membrane potential (Hille, 1992). Kawahara et al. (1987) also noted saturation of the *Necturus* BLM K^+ channel conductance with external $[K^+]$ in c/a patches.

Voltage dependence. Hyperpolarization increases nP_o. Such voltage sensitivity renders the channel susceptible to changes in membrane voltage, a potential regulator of the BLM K^+ conductance. On the BLM in the *Necturus* proximal tubule, hyperpolarization increased K^+ channel activity (Sackin and Palmer, 1987; Kawahara et al., 1987). In frog kidney, one study showed that nP_o increased with hyperpolarization (Kawahara, 1990), whereas

in another study, no voltage dependence of nP_o was observed (Hunter, 1991). In preliminary experiments using rabbit proximal tubule, we again found that hyperpolarization increases nP_o, although Parent et al. (1988) reported the opposite. Note that for the cloned renal K^+ channels, ROMK1 (Ho et al., 1993) and ROMK2 (Chepilko et al., 1995), which have not been detected in proximal tubule, nP_o decreases with hyperpolarization.

Selectivity and blockade. The channel is highly selective for K^+ over a number of cations (Na^+, Rb^+, Li^+, NH_4^+, and Cs^+) as well as over Cl^-. When K^+ in the patch pipette was replaced by these cations, c/a and i/o patches failed to show inward channel currents. Paired experiments in outside-out patches show that g_K:g_{Na} exceeds 30:1, and that the cation selectivity of the BLM K^+ channel is $K^+ >> Rb^+ \approx Cs^+ \approx NH_4^+ > Na^+ \approx Li^+$ (see Fig. 5). Detailed selectivity data are lacking in other studies on BLM K^+ channels in the proximal tubule, but more distal K^+ channels, including ROMK, conduct Rb^+. With Rb^+ in the patch pipette, g_{Rb}/g_K = 0.36 for ROMK2 (Chepilko et al., 1995). Under similar conditions, we did not observe inward Rb^+ currents through the BLM K^+ channel.

Like other types of K^+ channels (Hille, 1992), the BLM K^+ channel can conduct thallium. Indeed, the single channel conductance is higher for Tl^+ than it is for K^+ ($g^*_{in}Tl/g^*_{in}K = 1.2$). Since the reversal potential under biionic conditions (Tl^+ pipette, K^+ bath) is slightly positive, Tl^+ is also more permeant than K^+. This differs from ROMK2, in which Tl^+ is also more permeant than K^+ but the conductance for Tl^+ is less than that for K^+ ($g^*_{in}Tl/g^*_{in}K = 0.7$) (Chepilko et al., 1995). Thus, for the BLM K^+ channel, Tl^+ has a higher conductance and is more permeant than K^+.

Similar to other renal K^+ channels, this BLM K^+ channel is insensitive to tetraethylammonium. However, it is well known that the proximal tubule K^+ conductance can be inhibited by millimolar concentrations of Ba^{2+} (Sackin and Boulpaep, 1981) and the whole-cell conductance of the dissociated *Ambystoma* cells is barium sensitive (Segal et al., 1996). Outside-out patches from the BLM show that K^+ channel activity is inhibited by barium with a K_i of 460 μM at a command potential of −40 mV (see Fig. 7). Complete inhibition occurs at $[Ba^{2+}]_o$ = 10 mM.

Sensitivity to Nucleotides, Sulfonylureas, and Activation by Diazoxide

Nucleotides. The *Ambystoma* BLM K^+ channel is sensitive to ATP, albeit at millimolar levels. Since the first demonstration of an ATP-sensitive K (K_{ATP}) channel in cardiac muscle (Noma, 1983) and pancreatic cells (Cook and Hales, 1984), potassium channels inhibited by nucleotides have been described in a wide variety of tissues (Ashcroft and Ashcroft, 1990). In pancreatic β cells, K_{ATP} channels function in the regulation of insulin secretion. Ashcroft and Ashcroft (1990) have classified such inwardly rectifying K_{ATP} channels as Type I based on their exquisite sensitivity to ATP ($K_i \sim$ 10–100 μM) and sulfonylureas.

There is no doubt that K_{ATP} channels function primarily to couple cell metabolism to membrane potential (Ashcroft and Ashcroft, 1990), and perhaps to epithelial transport (Mauerer et al., 1998). Curiously, epithelial K_{ATP} channels appear to lack the exquisite sensitivity of Type I K_{ATP} channels, possibly for reasons discussed below. The proximal tubule BLM K^+ channel described in this study is reversibly inhibited by ATP with a K_i of 2.4 mM at pH 7.5. This is a reasonable operating point given that intracellular ATP levels in proximal tubule are 4–5 mM, and ATP levels have been shown to fall to ∼2 mM when transport is stimulated (Beck et al., 1991; Tsuchiya et al., 1992). The role of intracellular ATP in coupling channel activity to pump turnover is discussed in the companion paper.

It is likely that the intracellular ATP-binding site contains a motif that recognizes a spectrum of nucleotides since the channel is also reversibly inhibited by GTP, ITP, UTP, CTP, and TTP (see Fig. 8 *C*). This putative binding site recognizes NTPs, NDPs, and NMPs, but not the nucleosides themselves. Adenosine nucleotides exert significantly stronger inhibition than their nonadenosine counterparts, and the triphosphate of a given nucleoside is a better inhibitor than the diphosphate and the monophosphate. Since the binding of NDPs and even NMPs is effective, channel inhibition probably does not require hydrolysis. In contrast to the K_{ATP} channel on the apical membrane of principal cells (Wang and Giebisch, 1991), the inhibitory effect of the nucleotides is probably not critically dependent on Mg^{2+} since nucleotide sodium salts (free $Mg^{2+} \cong$ 25 μM) are as effective as the magnesium salts (free $Mg^{2+} \cong$ 1.3 mM).

Sulfonylureas. In cell-free patches, the *Ambystoma* and rabbit BLM K^+ channels are (variably) inhibited by submillimolar levels of glibenclamide, whereas native cell Type I K_{ATP} channels are sensitive to nanomolar concentrations of glibenclamide (Ashcroft and Ashcroft, 1990). Indeed, no renal and perhaps no epithelial K^+ channel has the sensitivity to sulfonylureas (or ATP) that Type I K_{ATP} channels possess. This may suggest that either Type I K_{ATP} channels are only found in specific tissues, or that associated molecules (e.g., the sulfonylurea receptor) conferring sulfonylurea sensitivity are cell specific. In this regard, it is of interest that all but one of the cloned K_{ATP} channels fail to exhibit the degree of sulfonylurea sensitivity seen in the native β cell K_{ATP} channels. The exception is the K_{ATP} channel composed of Kir6.2 and the sulfonylurea receptor itself (Inagaki et al., 1995).

In the kidney, cloned ROMK channels are ATP regulated in the sense that they rundown in the absence of ATP, but also have a much lower (if any) sensitivity to ATP and sulfonylureas (Ho et al., 1993; Zhou et al., 1994). At least on Northern analysis, the kidney also appears to lack SUR1 (Inagaki et al., 1995), which may partially account for the decrease in glibenclamide sensitivity. Of note, the renal K^+ channel ROMK2 appears to be sensitive to glibenclamide when coexpressed with the cystic fibrosis transmembrane conductance regulator, but becomes much less sensitive after PKA phosphorylation of the patch (McNicholas et al., 1996). Since phosphorylation by PKA activates the BLM K_{ATP} channel (Mauerer et al., 1998), it may be that high current patches are already highly phosphorylated, and thus relatively insensitive to glibenclamide. That glibenclamide inhibition of the BLM K_{ATP} channel appears significantly more potent in cell-attached patches with smaller currents is consistent with this idea.

Diazoxide. Diazoxide is a benzothiadiazine K channel opener (KCO) that activates several types of K_{ATP} channels. In many tissues, it is thought that activation by KCOs requires Mg-ATP (Edwards and Weston, 1993; Ashcroft and Ashcroft, 1990), as illustrated for the BLM K^+ channel in Fig. 10. Diazoxide also does not alter the requirement for Mg-ATP to prevent BLM K^+ channel rundown (see below). Indeed, diazoxide can be inhibitory in the absence of Mg-ATP, perhaps by accelerating channel rundown (Kozlowski et al., 1989). Therefore, it is not likely that diazoxide exerts its effect on the rundown site of the BLM K^+ channel.

For both the frog muscle K_{ATP} channel and the *Ambystoma* BLM K^+ channel, KCOs lose their effectiveness at high (5–10 mM) intracellular [ATP]. This reciprocal effect on channel activity suggests a competitive interaction between KCOs and nucleotides. The activation by KCOs in the frog skeletal K_{ATP} channel is not Mg^{2+} dependent and, like the BLM K^+ channel, does not occur in the absence of ATP. Further studies may thus show that diazoxide opens the BLM K^+ channel by a mechanism similar to that recently proposed for KCO activation of the skeletal muscle K_{ATP} channel (Forestier et al., 1996).

TABLE III

Rundown for ROMK1 Compared with the BLM K^+ Channel

Nucleotide	Free Mg^{2+}	ROMK1 rundown*	BLM K^+ rundown
0.2 mM ATP	1 mM Mg^{2+}	No	No
0.2 mM ATP-γS	1 mM Mg^{2+}	?	Yes
ATP-free	1 mM Mg^{2+}	Yes	Yes
0.2 mM ATP	Mg^{2+}-free	Yes	Yes
ATP-free	Mg^{2+}-free	No	Yes

*As expressed in *Xenopus* oocytes; data from McNicholas et al. (1994).

Rundown of the BLM K^+ Channel

A hallmark of K_{ATP} channels is that they exhibit the phenomenon of rundown, a gradual loss of activity when the membrane patch is deprived of cytosolic ATP. As first noted by Findlay and Dunne (1986), rundown is "a paradoxical situation in that K^+ channels that are inhibited by intracellular ATP require intracellular ATP to retain the ability to open." In a recent study on frog proximal tubule cells (Robson and Hunter, 1997), washout of intracellular ATP reduced the whole-cell barium-sensitive conductance by ~60% over 10 min. Inclusion of 2 mM ATP in the patch pipette not only prevented this rundown, but the barium-sensitive conductance increased by 54% over 10 min.

Accordingly, the BLM K^+ channel runs down in the absence of ATP, and low concentrations of ATP (100–200 μM) are required to prevent or rescue channel rundown in cell-free patches. Once rundown has begun, application of ATP will restore channel activity, but the ATP-restorable current decreases as the time between rundown and ATP application lengthens. The BLM K^+ channel specifically requires Mg-ATP to support activity as rundown occurs if either ATP, Mg^{2+}, or both are removed (see Table III). Typically, both Mg^{2+} and ATP are required to prevent rundown in K_{ATP} channels (Ashcroft and Ashcroft, 1990). Mg^{2+} is required as a cofactor, as channel rundown occurs in a Mg^{2+}-free solution despite the presence of Na-ATP. Free Mg^{2+} concentrations as low as 200 nM are sufficient to prevent BLM K^+ channel rundown in the presence of ATP. The possibility that free Mg^{2+} itself (rather than the Mg-ATP complex) plays a distinct role in the rundown of the BLM K^+ channel cannot be excluded, but is difficult to test since rundown occurs if either Mg^{2+} or ATP is removed. Interestingly, free Mg^{2+} itself (≥10 μM) can prevent rundown of $K_{ir}2.1$, an ATP-insensitive inward rectifier (Fakler et al., 1994).

Paradoxically, removal of free Mg^{2+} nearly abolishes rundown of K_{ATP} in cultured CRI-G1 insulin-secreting cells (Kozlowski and Ashford, 1990) and partially inhibits rundown of ATP-regulated ROMK1 channels excised in an ATP-free bath (McNicholas et al., 1994). The latter effect is presumed to occur via the inhibition of a Mg^{2+}-dependent phosphatase (McNicholas et al., 1994). Thus, removal of Mg^{2+} inhibits rundown in ROMK1, but actually produces rundown in the BLM K^+ channel (see Fig. 9 *C*). We conclude that the Mg^{2+}-dependent phosphatase thought to be involved in the rundown of ROMK1 (McNicholas et al., 1994) does not mediate rundown of the BLM K^+ channel.

ATP can serve as a substrate in hydrolysis reactions

mediated by an ATPase and in phosphorylation reactions mediated by a kinase. We asked whether phosphorylation itself (without hydrolysis) can prevent BLM K^+ channel rundown, as has been proposed for other channels, including ROMK1 (McNicholas et al., 1994). To address this issue, we used ATP-γS, a poorly hydrolyzable ATP analogue that is an effective substrate for most kinases (e.g., PKA) in (thio)phosphorylation reactions (Eckstein, 1985). Similar to results reported for the cell K_{ATP} channel (Ohno-Shosaku et al., 1987), our findings (see Fig. 9 and Table III) indicate that ATP-γS cannot substitute for ATP in sustaining channel activity, whereas all hydrolyzable nucleoside triphosphates we tested do prevent or rescue rundown. The corresponding nucleoside diphosphates were also ineffective.

In summary, rundown of the BLM K^+ channel in excised patches seems to be prevented by a high affinity nucleotide binding site, which hydrolyzes nucleoside triphosphates in the presence of Mg^{2+}. Rundown is prevented by ATP even in the presence of high concentrations of a protein kinase inhibitor, strongly suggesting that typical protein phosphorylation processes alone are insufficient to prevent/rescue channel rundown. Fakler et al. (1994) obtained similar results in $K_{ir}2.1$ channels.

Comparison with Other Studies

Gögelein and Greger (1987*b*) found a very weak inward rectifier K^+ channel on the lateral membrane of rabbit proximal straight tubule. In symmetrical KCl with 1 mM Mg^{2+} in the bath, this channel had a limiting g_{in} of ~45 pS and a limiting g_{out} of ~40 pS. In contrast to the results of the present study, their channel's open probability did not increase with hyperpolarization, and nP_o was unaffected by Ca^{2+} (<1 nM–1 μM) applied to inside-out patches (Mauerer et al., 1998). They did not observe channel rundown in excised patches, the channel was tetraethylammonium sensitive, and the effect of ATP was not tested. Thus, it is not likely that their channel was the BLM K^+ channel we find in *Ambystoma* proximal tubule.

Kawahara et al. (1987) found a 31-pS K^+ channel in 42% of cell-attached patches made on the BLM of *Necturus* proximal tubule. They also found saturation of inward channel conductance at ~50 pS (compared with ~35 pS for *Ambystoma*) and an apparent K_m of 65.5 mM (compared with 77 mM in *Ambystoma*). Whereas we observed inward rectification for all [K], their I-V plots were restricted to inward currents. Similar to our findings in *Ambystoma*, the K^+ channel in *Necturus* showed high selectivity (P_K:P_{Na} ≈ 10:1 in *Necturus* versus ≈ 30:1 in *Ambystoma*), channel activity increased with hyperpolarization, and external Na^+ did not influence channel behavior. They also found that hyperpolarization did not affect channel open time; rather, the increase in nP_o was due to shortening a closed state lifetime. Significantly, Kawahara et al. (1987) were unable to maintain channel activity in excised patches, stating that "patches became unstable and noisy after excision." It is likely that this was channel rundown since this description is reminiscent of the channel "choking" and rundown we observe in an ATP-free bath.

Similarly, Sackin and Palmer (1987) observed two BLM K^+ channels in *Necturus*, a short open-time channel that they studied in detail, and a long open-time channel that disappeared after excision, perhaps because of rundown. The short open-time channel is different from the BLM K^+ channel of *Ambystoma* since it was nonrectifying and did not rundown when excised in an ATP-free bath. The long open-time channel was thought to be the same as that studied in cell-attached patches by Kawahara et al. (1987), and probably corresponds to the BLM K^+ channel in *Ambystoma* except the channel in *Necturus* had a mean open time of ~60 ms, much longer than that seen in our study.

Parent et al. (1988) made cell-attached patches on rabbit BLM and found an inward-rectifier K^+ channel that had different properties than both the *Ambystoma* BLM K^+ channels in the present study. Their voltage dependence was opposite to ours, as they concluded that hyperpolarization induced a long closed state.

Hunter (1991) made cell-attached patches on the BLM of single frog proximal tubule cells and found only one kind of K^+ channel, an inward rectifier with an inward g_{slope} = 32.4 pS, and an outward g_{chord} = 6.2 pS at +80 mV, similar to the one we studied on the BLM of *Ambystoma* proximal tubule. Depolarization reduces the macroscopic BLM K^+ conductance and single-channel conductance in both preparations. A Boltzmann fit of the *g*–V curves (rederived using Fig. 5 of Hunter, 1991, and the inset of Fig. 3 *B* in the present study) shows a $V_{1/2}$ = +31.7 mV and a width of 14.5 mV for the BLM K^+ channel in c/a patches of frog, compared with a $V_{1/2}$ = −14.9 mV and a width of 21.3 mV for the BLM K^+ channel in i/o patches of *Ambystoma*. Thus, the sensitivity of conductance versus voltage is such that there is an e-fold change in g per 14.5 mV in frog (c/a), and per 21.3 mV in *Ambystoma* (i/o). The discrepancy in $V_{1/2}$ may be due to different experimental conditions and levels of cytosolic Mg^{2+}. Hunter (1991) also reported that the addition of glucose and/or alanine did not affect BLM K^+ channel activity in the frog cells. Although addition of alanine depolarized V_m > 30 mV, he was unable to explain the repolarization of the BLM under his experimental conditions. In contrast, the *Ambystoma* BLM K^+ channel under discussion is activated by these substrates, which can explain the repolarization of the BLM (Mauerer et al., 1998). In a

TABLE IV

Contribution of the K^+ Conductance to the BLM Conductance of Proximal Tubule

Species	g	NP_o	f	A	G_K	G_{BLM}	G_K/G_{BLM}
	pS			*10^{-8}cm²*	*μS/cm²*	*μS/cm²*	
Necturus	31.2*	0.14*	1.0*‡	1.3*	33.6*	33–59§	0.57–1.00
			0.42*		14.1		0.24–0.43
Rana	5.6‖	0.22‖	0.62‖	1.57‖	48‖	33–59§	0.81–1.45
						51.3¶	0.94
Rabbit	10**	0.06**	1.0‡‡	1.0**	100**	714§§	0.14
Ambystoma	4‖‖	0.20‖‖	0.986‖‖	1.77‖‖	44.6‖‖	51.3¶	0.87

*From Kawahara et al., 1987; cell-attached at 0 mV; ‡assumed in the calculation in Kawahara et al. (1987), despite finding f = 0.42; §from Maunsbach and Boulpaep (1984), for *Necturus*; ‖from Hunter (1991), cell attached at 0 mV; ¶from Maunsbach and Boulpaep (1984), for *Ambystoma*; **from Parent et al. (1988), cell-attached at −50 mV; ‡‡presumed, since data not given in Parent et al. (1988); §§from Lapointe et al. (1984); ‖‖present study.

recent follow-up study, Robson and Hunter (1997) proposed that, based on differential sensitivity to barium and quinidine, the frog cells have two separate K^+ conductances. The inwardly rectifying conductance that was inhibited by both agents appears similar to the *Ambystoma* BLM K_{ATP} channel, although direct sensitivity to ATP or glibenclamide was not tested in their study.

Tsuchiya et al. (1992) found an ATP-sensitive K^+ channel in five patches made on the BLM of nonperfused rabbit S1 and S2 segments. With 145 mM K^+ in the patch pipette and a bath containing 140 mM Na^+ and 5 mM K^+, they reported an inward g_{slope} = 56 pS, although an I-V plot was not given. In c/a patches at a command potential of 0 mV, they found a baseline nP_o of 0.72, much higher than that found in the present study and the two studies in which perfused tubules were patched (see below) (Hurst et al., 1993; Beck et al., 1993). Although 1 mM ATP applied to the cytoplasmic side of an inside-out patch reversibly reduced nP_o by 77% (from 0.70 to 0.16), the sensitivity of the basolateral conductance was reduced in a perfused tubule when 1 mM ATP was added to the bath.

Beck et al. (1993) were the first to patch clamp the BLM of (collagenase-treated) perfused rabbit proximal tubules, and found a K^+ channel whose activity correlated to transport activity. This channel showed inward rectification in c/a patches (with g_{in} = 61 pS and g_{out} = 17 pS) and P_o was voltage independent. In a follow-up study (Hurst et al., 1993), the same group showed that 2 mM ATP (i/o) inhibited channel activity by ~80% and 100 μM diazoxide (c/a) effectively opened this BLM K^+ channel.

The ROMK family of K^+ channels is, to date, the only cloned ATP-regulated renal K^+ channel (Ho et al., 1993). The ROMK1 channel cloned from rat kidney is an inwardly rectifying K^+ channel with g_{in} = 39 pS and a high open probability (0.8–0.9) at voltages more depolarized than −60 mV, and is not activated by hyperpolarization. ROMK1 exhibits channel rundown when membrane patches are excised in ATP-free bath, although ROMK1 is not sensitive to ATP or glibenclamide (Ho et al., 1993). In situ hybridization studies show that transcripts (mRNA) for ROMK are absent

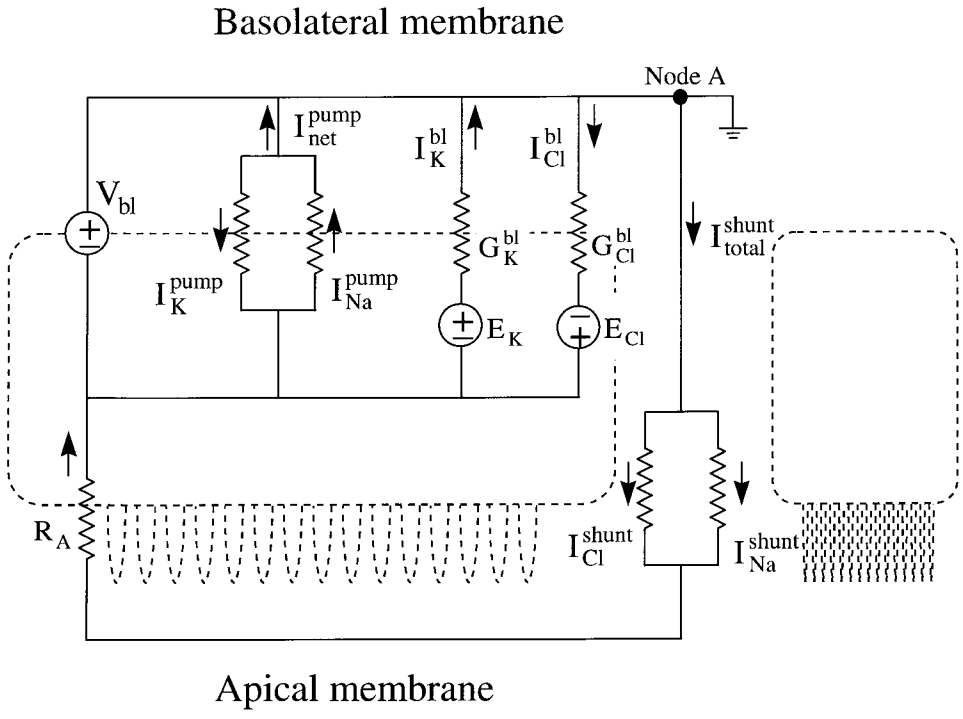

FIGURE 11. Equivalent electrical cell/circuit. Adjacent proximal tubule cells are outlined as dashed lines, and the equivalent circuit discussed in the text is diagrammed on the left. The basolateral membrane potential is denoted by voltage source V_{bl}. The current produced by the Na,K-ATPase pump, I_{net}^{pump} is given by $I_{Na}^{pump} + I_K^{pump}$. Basolateral ion channel currents are shown as their Thévenin equivalents with their conductances, G_K^{bl} and G_{Cl}^{bl}, represented by the equivalent resistor, in series with their Nernst potentials, E_K and E_{Cl}, respectively. The paracellular current, I_{total}^{shunt} is represented by $I_{Na}^{shunt} + I_{Cl}^{shunt}$. R_A is the resistance of the apical membrane. Kirchoff's current law at Node A is given by Eq. 11.

from the proximal tubule (Lee and Hebert, 1995). Combined with the differences in mechanism of channel rundown (see above and Table III), it is highly unlikely that the BLM K^+ channel is ROMK1, although it may be within the same family of inwardly rectifying K^+ channels with two transmembrane domains (Ho et al., 1993; Kubo et al., 1993).

Contribution of the BLM K^+ Channel to Total BLM Conductance

The component of BLM conductance (G_{BLM}) due to the BLM K^+ channel (G_K) can be estimated as:

$$G_K = \frac{g \cdot nP_o \cdot f}{a}, \quad (10)$$

where g is the "physiologic" single channel conductance, n is the average number of channels in a patch, P_o is the mean open time of one channel, f is the incidence of finding a channel in the patch, and a is the area of the membrane patch.

In the present study, the conductance (g) for outward currents was ~4 pS, the average nP_o extrapolated to 0 mV was 0.20, and channel activity was found in 98.6% of patches. Given that the average inner diameter of our patch pipette was 1.5 μm, the minimal membrane area of a patch is 1.77 μm^2. Using these estimates in *Ambystoma*, the value for G_K is (4 pS*0.20*0.986)/1.77 μm^2 = 0.446 pS/μm^2 or 44.6 S/cm^2 (R_K = 22.4 k$\Omega \cdot cm^2$). Considering the estimate of G_{BLM} = 51.3 μS/cm^2 (R_{BLM} = 19.5 k$\Omega \cdot cm^2$) in *Ambystoma* proximal tubule (Maunsbach and Boulpaep, 1984), G_K/G_{BLM} = 44.6/51.3 = 0.87. Thus, under the conditions used in our experiments, G_K may account for 87% of G_{BLM}. However, to the extent that the area of the membrane patch is larger than our estimate, G_K will be smaller.

The basolateral membrane area of dissociated *Ambystoma* proximal tubule cells exhibits less infoldings than these cells in situ (Segal et al., 1996). Assuming a whole-cell membrane capacitance of ~120 pF (Segal et al., 1996) and a specific capacitance of 1 pF per 100 μm^2, we can estimate that the surface of a single isolated cell is ~12,000 μm^2. Using a BLM surface area of 10,000 μm^2 (100 × 10^{-6} cm^2) and a G_{BLM} = 51.3 μS/cm^2, the total BLM conductance is 5.13 nS. Using the transport number G_K/G_{BLM} of 0.87 from Table IV, G_K = 4.46 nS. Despite possible changes in membrane area (e.g., due to membrane recycling) and/or channel density that could occur in the dissociated cells over time, this is a reasonable estimate since perforated-patch whole-cell studies with KCl pipette and NaCl bath (E_K = −84 mV) show current that reverses at V_m = −40 mV with ~240 pA of outward current at 0 mV command potential, and a whole-cell conductance of 6 nS. Thus, the total BLM conductance is 5.13 nS, of which 4.46 nS is K conductance, and the total apical conductance is 0.87 nS (the difference of 6–5.13).

Similar comparisons between G_K derived from single-channel data and G_{BLM} based on cable analysis are shown in Table IV for *Necturus*, *Rana*, and rabbit proximal tubule, respectively. With the exception of the rabbit, the transport numbers show that the BLM conductance of all other species is dominated by K^+ and, specifically for *Ambystoma*, K_{ATP} channels. From this information, one can estimate the K^+ channel density on the BLM of dissociated *Ambystoma* proximal tubule cells. If P_o was unity, the number of channels would be given by 4.46 nS/4 pS = 1,115 channels. However, since P_o = 0.05, the number of K^+ channels on the BLM is ~22,300 per cell; a channel density of 2.23 channels/μm^2. Using the estimate of membrane patch area of 1.77 μm^2, one would expect on average approximately four channels per patch, in good agreement with our experience.

Physiological Role of the BLM K_{ATP} Channel

The task of the proximal tubule under physiologic conditions is to effect transport; i.e., to maintain ionic flux in the direction of reabsorption. The electrochemical difference across the BLM of proximal tubule, given by $V_{bl} - E_K$, is an invariably positive driving force promoting K^+ efflux (Boulpaep, 1979). The presence of other conductances in the BLM with reversal potentials less negative than E_K provides a nonzero difference between E_K and V_{bl} that maintains K efflux. The BLM Na^+,K^+-ATPase pump loads the cell with two K^+ ions to effect the transcellular transport of three Na^+ ions. An efflux pathway for K^+ is necessary to recycle K^+ across the BLM, thus permitting continuous operation of the pump. Pump activity and the opening of these K^+ channels hyperpolarize the BLM, favoring apical Na^+ entry. An interesting contrast is that the negative shift in membrane potential consequent to the opening of K_{ATP} channels tends to depress cell function in excitable cells, but tends to promote transport in epithelia. The magnitude of BLM K^+ efflux must match the K^+ current of the pump. The regulatory effects of hyperpolarization and intracellular ATP levels on the BLM K_{ATP} channels thus subserve this role.

This system of a variable BLM K^+ conductance coupled to changes in pump rate in a single cell has further implications when extrapolated to the level of an epithelium with a paracellular shunt pathway. Such an epithelial model should include all current pathways (see Fig. 11, adapted from Fig. 5 of Sackin and Boulpaep, 1983); namely, (*a*) the active Na^+ and K^+ pump currents, (*b*) the basolateral K^+ leak current, (*c*) the other basolateral leak currents, principally carried by Cl^-, and (*d*) the shunt current carried by Cl^- and, to a

lesser extent, by Na^+. In this equivalent electrical cell/circuit, Kirchoff's current law at node A gives

$$I_{net}^{pump} + I_{K}^{bl} - I_{Cl}^{bl} - I_{total}^{shunt} = 0\,, \qquad (11)$$

where $I_{net}^{pump} = I_{Na}^{pump} - I_{K}^{pump}$, $I_{K}^{bl} = (V_{bl} - E_K) \cdot G_K^{bl}$, I_{Cl}^{bl} is the transcellular component of Cl^- absorption, and $I_{total}^{shunt} = I_{Cl}^{shunt} + I_{Na}^{shunt}$ (i.e., the sum of the paracellular component of Cl^- absorption and any Na^+ backleak). If the outward current through BLM K channels could be exactly matched to I_K^{pump}, then Eq. 11 becomes

$$I_{Na}^{pump} - I_{Cl}^{bl} - (I_{Cl}^{shunt} + I_{Na}^{shunt}) = 0\,. \qquad (12)$$

When Eq. 12 is satisfied, all actively transported Na^+ is accompanied by Cl^- absorption (sum of transcellular and paracellular), except for the backleak, I_{Na}^{shunt}. Under these optimal conditions, the proximal tubule accomplishes NaCl reabsorption at maximum efficiency.

Note that if G_K^{bl} did not increase with pump rate, I_K^{bl} would rise only slightly due to the small increase in driving force. Under these conditions, $I_{Na}^{pump} > I_{Cl}^{bl} + (I_{Cl}^{shunt} + I_{Na}^{shunt})$ and the efficiency of NaCl reabsorption deteriorates. That is, the incremental increase in NaCl reabsorption would be less than that of the pump. Therefore, the tight linkage between the Na^+,K^+-ATPase pump and the K^+ leak through the BLM K_{ATP} channels is especially important in leaky epithelia that absorb large, fluctuating quantities of NaCl such as the proximal tubule. The regulation of the BLM K_{ATP} channels and how they are coupled to the pump during transport is the subject of the companion paper (Mauerer et al., 1998).

This work is dedicated to the memory of Dr. Roman Mauerer (father of Ulrich Mauerer), who passed away during the preparation of the manuscript. The authors thank Ms. Christine Macol for excellent technical assistance.

This work was supported by grant DK-17433 from the National Institutes of Health (NIH). Dr. A. Segal is a recipient of a Physician-Scientist Award from the NIH (DK-02103).

Original version received 16 January 1997 and accepted version received 30 October 1997.

REFERENCES

Aguilar-Bryan, L., C.G. Nichols, S.W. Wechsler, J.P. Clement IV, A.E. Boyd III, G. Gonzalez, H. Herrera-Sosa, K. Nguy, J. Bryan, and D.A. Nelson. 1995. Cloning of the beta cell high-affinity sulfonylurea receptor: a regulator of insulin secretion. *Science.* 268: 423–426.

Ashcroft, S.J., and F.M. Ashcroft. 1990. Properties and functions of ATP-sensitive K-channels. *Cell Signal.* 2:197–214.

Balaban, R.S., L.J. Mandel, S.P. Soltoff, and J.M. Storey. 1980. Coupling of active ion transport and aerobic respiratory rate in isolated renal tubules. *Proc. Natl. Acad. Sci. USA.* 77:447–451.

Beck, J.S., A.M. Hurst, J.Y. Lapointe, and R. Laprade. 1993. Regulation of basolateral K channels in proximal tubule studied during continuous microperfusion. *Am. J. Physiol.* 264:F496–F501.

Beck, J.S., S. Breton, H. Mairbäurl, R. Laprade, and G. Giebisch. 1991. Relationship between sodium transport and intracellular ATP in isolated perfused rabbit proximal convoluted tubule. *Am. J. Physiol.* 261:F634–F639.

Boim, M.A., K. Ho, M.E. Shuck, M.J. Bienkowski, J.H. Block, J.L. Slightom, Y. Yang, B.M. Brenner, and S.C. Hebert. 1995. ROMK inwardly rectifying ATP-sensitive K^+ channel. II. Cloning and distribution of alternative forms. *Am. J. Physiol.* 268:F1132–F1140.

Boulpaep, E.L. 1976. Electrical phenomena in the nephron. *Kidney Int.* 9:88–102.

Boulpaep, E.L. 1979. Electrophysiology of the kidney. *In* Transport Across Biological Membranes. G. Giebisch, D.C. Tosteson, and H.H. Ussing, editors. Springer-Verlag, Berlin, Germany. 97–144.

Chepilko, S., H. Zhou, H. Sackin, and L.G. Palmer. 1995. Permeation and gating properties of a cloned renal K^+ channel. *Am. J. Physiol.* 268:C389–C401.

Colquhoun, D., and F.J. Sigworth. 1983. Fitting and statistical analysis of single-channel records. *In* Single-Channel Recording. B. Sakmann and E. Neher, editors. Plenum Publishing Corp., New York. 191–263.

Cook, D.L., and C.N. Hales. 1984. Intracellular ATP activity directly blocks K^+ channels in pancreatic B-cells. *Nature.* 311:271–273.

Davis, C.W., and A.L. Finn. 1982. Sodium transport inhibition by amiloride reduces basolateral membrane potassium conductance in tight epithelia. *Science.* 216:525–527.

Eckstein, F. 1985. Nucleoside phosphorothioates. *Annu. Rev. Biochem.* 54:367–402.

Edwards, G., and A.H. Weston. 1995. Pharmacology of the potassium channel openers. *Cardiovasc. Drugs Ther.* 9(Suppl. 2):185–193.

Edwards, G., and A.H. Weston. 1993. The pharmacology of ATP-sensitive potassium channels. *Annu. Rev. Pharmacol. Toxicol.* 33: 597–637.

Fabiato, A., and F. Fabiato. 1979. Calculator programs for computing the composition of the solutions containing multiple metals and ligands used for experiments in skinned muscle cells. *J. Physiol. Paris.* 75:463–505.

Fakler, B., U. Brandle, E. Glowatzki, H.P. Zenner, and J.P. Ruppersberg. 1994. Kir2.1 inward rectifier K^+ channels are regulated independently by protein kinases and ATP hydrolysis. *Neuron.* 13: 1413–1420.

Ficker, E., M. Taglialatela, B.A. Wible, C.M. Henley, and A.M. Brown. 1994. Spermine and spermidine as gating molecules for inward rectifier K^+ channels. *Science.* 266:1068–1072.

Findlay, I., and M.J. Dunne. 1986. ATP maintains ATP-inhibited K^+ channels in an operational state. *Pflügers Arch.* 407:238–240.

Forestier, C., J. Pierrard, and M. Vivaudou. 1996. Mechanism of action of K channel openers on skeletal muscle KATP channels. *J. Gen. Physiol.* 107:489–502.

Gögelein, H., and R. Greger. 1987*a*. Potassium-selective channels in the basolateral and luminal membranes of the late proximal tubule of the rabbit kidney. *Pflügers Arch.* 410:288–295.

Gögelein, H., and R. Greger. 1987*b*. Properties of single K^+ channels in the basolateral membrane of rabbit proximal straight tubules. *Pflügers Arch.* 410:288–295.

Goldman, D.E. 1943. Potential, impedance, and rectification in membranes. *J. Gen. Physiol.* 27:37–60.

Gunter-Smith, P.J., E. Grasset, and S.G. Schultz. 1982. Sodium-coupled amino acid and sugar transport by Necturus small intestine: an equivalent circuit analysis of a rheogenic cotransport system. *J. Membr. Biol.* 66:25–39.

Hamill, O., E. Marty, E. Neher, B. Sakmann, and F. Sigworth. 1981. Improved patch-clamp techniques for high resolution current recording from cells and cell-free membrane patches. *Pflügers Arch.* 391:85–100.

Hebert, S.C., and K. Ho. 1994. Structure and functional properties of an inwardly rectifying ATP-regulated K^+ channel from rat kidney. *Renal Physiol. Biochem.* 17:143–147.

Hille, B. 1992. Ionic Channels of Excitable Membranes. 2nd edition. Sinauer Associates, Inc., Sunderland, MA. 607 pp.

Ho, K., C.G. Nichols, W.J. Lederer, J. Lytton, P.M. Vassilev, M.V. Kanazirska, and S.C. Hebert. 1993. Cloning and expression of an inwardly rectifying ATP-regulated potassium channel. *Nature.* 362:31–38.

Hodgkin, A.L., and B. Katz. 1949. The effect of sodium ions on the electrical activity of the giant axon of the squid. *J. Physiol. (Camb.).* 108:37–77.

Horie, M., H. Irisawa, and A. Noma. 1987. Voltage-dependent magnesium block of adenosine-triphosphate-sensitive potassium channel in guinea-pig ventricular cells. *J. Physiol. (Camb.).* 387: 251–272.

Hunter, M. 1991. Potassium-selective channels in the basolateral membrane of single proximal tubule cells of frog kidney. *Pflügers Arch.* 418:26–34.

Hurst, A.M., J.S. Beck, R. Laprade, and J.Y. Lapointe. 1993. Na^+ pump inhibition downregulates an ATP-sensitive K^+ channel in rabbit proximal convoluted tubule. *Am. J. Physiol.* 264:F760–F764.

Inagaki, N., T. Gonoi, J.P. Clement IV, N. Namba, J. Inazawa, G. Gonzalez, L. Aguilar-Bryan, S. Seino, and J. Bryan. 1995. Reconstitution of I_{KATP}: an inward rectifier subunit plus the sulfonylurea receptor. *Science.* 270:1166–1170.

Kawahara, K. 1990. A stretch-activated K^+ channel in the basolateral membrane of Xenopus kidney proximal tubule cells. *Pflügers Arch.* 415:624–629.

Kawahara, K., M. Hunter, and G. Giebisch. 1987. Potassium channels in *Necturus* proximal tubule. *Am. J. Physiol.* 253:F488–F494.

Koefoed Johnsen, V., and H. Ussing. 1958. The nature of the frog skin potential. *Acta Physiol. Scand.* 42:298–308.

Kozlowski, R.Z., C.N. Hales, and M.L. Ashford. 1989. Dual effects of diazoxide on ATP-K^+ currents recorded from an insulin-secreting cell line. *Br. J. Pharmacol.* 97:1039–1050.

Kozlowski, R.Z., and M.L. Ashford. 1990. ATP-sensitive K^+-channel run-down is Mg^{2+} dependent. *Proc. R. Soc. Lond. B Biol. Sci.* 240: 397–410.

Kubo, Y., T.J. Baldwin, Y.N. Jan, and L.Y. Jan. 1993. Primary structure and functional expression of a mouse inward rectifier potassium channel. *Nature.* 362:127–133.

Lapointe, J.Y., R. Laprade, and J. Cardinal. 1984. Transepithelial and cell membrane electrical resistances of the rabbit proximal convoluted tubule. *Am. J. Physiol.* 247:F637–F649.

Lee, W.S., and S.C. Hebert. 1995. ROMK inwardly rectifying ATP-sensitive K^+ channel. I. Expression in rat distal nephron segments. *Am. J. Physiol.* 268: F1124–F1131.

Matsuda, H., A. Saigusa, and H. Irisawa. 1987. Ohmic conductance through the inwardly rectifying K channel and blocking by internal Mg. *Nature.* 325:156–159.

Matsumura, Y., B. Cohen, W.B. Guggino, and G. Giebisch. 1984. Regulation of the basolateral potassium conductance of the *Necturus* proximal tubule. *J. Membr. Biol.* 79:153–161.

Mauerer, U.R., E.L. Boulpaep, and A.S. Segal. 1998. Regulation of an inwardly rectifying adenosine triphosphate–sensitive K^+ channel in the basolateral membrane of renal proximal tubule. *J. Gen. Physiol.* 111:161–180.

Maunsbach, A.B., and E.L. Boulpaep. 1984. Quantitative ultrastructure and functional correlates in proximal tubule of *Ambystoma* and *Necturus*. *Am. J. Physiol.* 246:F710–F724.

McNicholas, C.M., W.B. Guggino, E.M Schwiebert, S.C. Hebert, G. Giebisch, and M.E. Egan. 1996. Sensitivity of a renal K^+ channel (ROMK2) to the inhibitory sulfonylurea compound glibenclamide is enhanced by coexpression with the ATP-binding cassette transporter cystic fibrosis transmembrane regulator. *Proc. Natl. Acad. Sci. USA.* 93:8083–8088.

McNicholas, C.M., W. Wang, K. Ho, S.C. Hebert, and G. Giebisch. 1994. Regulation of ROMK1 K^+ channel activity involves phosphorylation processes. *Proc. Natl. Acad. Sci. USA.* 91:8077–8081.

Noma, A. 1983. ATP-regulated K^+ channels in cardiac muscle. *Nature.* 305:147–148.

Ohno-Shosaku, T., B.J. Zunkler, and G. Trube. 1987. Dual effects of ATP on K^+ currents of mouse pancreatic beta-cells. *Pflügers Arch.* 408:133–138.

Parent, L., J. Cardinal, and R. Sauve. 1988. Single-channel analysis of a K channel at basolateral membrane of rabbit proximal convoluted tubule. *Am. J. Physiol.* 254:F105–F113.

Robson, L., and M. Hunter. 1997. Two K^+-selective conductances in single proximal tubule cells isolated from frog kidney are regulated by ATP. *J. Physiol. (Camb.).* 500:605–616.

Romero, P.J. 1978. Is the Ca^{2+}-sensitive K^+ channel under metabolic control in human red cells? *Biochim. Biophys. Acta.* 507:178–181.

Sackin, H., and E.L. Boulpaep. 1981. Isolated perfused salamander proximal tubule. II. Monovalent ion replacement and rheogenic transport. *Am. J. Physiol.* 241:F540–555.

Sackin, H., and E.L. Boulpaep. 1983. Rheogenic transport in the renal proximal tubule. *J. Gen. Physiol.* 82:819–851.

Sackin, H., and L.G. Palmer. 1987. Basolateral potassium channels in renal proximal tubule. *Am. J. Physiol.* 253:F476–F487.

Segal, A.S., E.L. Boulpaep, and A.B. Maunsbach. 1996. A novel preparation of dissociated renal proximal tubule cells that maintain epithelial polarity in suspension. *Am. J. Physiol.* 270:C1843–C1863.

Siebens, A.W., and W.F. Boron. 1987. Effect of electroneutral luminal and basolateral lactate transport on intracellular pH in salamander proximal tubules. *J. Gen. Physiol.* 90:799–831.

Sigworth, F.J., and S.M. Sine. 1987. Data transformations for improved display and fitting of single-channel dwell time histograms. *Biophys. J.* 52:1047–1054.

Spruce, A.E., N.B. Standen, and P.R. Stanfield. 1985. Voltage-dependent ATP-sensitive potassium channels of skeletal muscle membrane. *Nature.* 316:736–738.

Standen, N.B., J.M. Quayle, N.W. Davies, J.E. Brayden, Y. Huang, and M.T. Nelson. 1989. Hyperpolarizing vasodilators activate ATP-sensitive K^+ channels in arterial smooth muscle. *Science.* 245: 177–180.

Tsuchiya, K., W. Wang, G. Giebisch, and P.A. Welling. 1992. ATP is a coupling modulator of parallel Na,K-ATPase-K-channel activity in the renal proximal tubule. *Proc. Natl. Acad. Sci. USA.* 89:6418–6422.

Wang, W., and G. Giebisch. 1991. Dual effects of adenosine triphosphate on the apical small conductance K^+ channel of the rat cortical collecting duct. *J. Gen. Physiol.* 98:35–61.

Woodhull, A.M. 1973. Ionic blockage of sodium channels in nerve. *J. Gen. Physiol.* 61:687–708.

Zhou, H., S.S. Tate, and L.G. Palmer. 1994. Primary structure and functional properties of an epithelial K channel. *Am. J. Physiol.* 266:C809–C824.